PHASE-LOCKING STABILITY OF A QUASI-SINGLE-CYCLE PULSE

by

NATHAN BODNAR
B.S. University of Central Florida, 2010

A thesis submitted in partial fulfillment of the requirements
for the degree of Master of Science
in the College of Optics and Photonics
at the University of Central Florida
Orlando, Florida

Fall Term
2012

ABSTRACT

There is increasing interest in the generation of very short laser pulses, even down to attosecond (10^{-18} s) durations. Laser systems with femtosecond pulse durations are needed for these applications. For many of these applications, positioning of the maximum electric field within the pulse envelope can affect the outcome. The peak of the electric field relative to the peak of the pulse is called the Carrier Envelope Phase (CEP). Controlling the position of the electric field becomes more important when pulse duration approaches single-cycle.

This thesis focuses on the stabilization of a quasi-single-cycle laser facility. Improvements to this already-established laser facility, HERACLES (High Energy, Repetition rate Adjustable, Carrier-Locked-to-Envelope System) described in this thesis include a stabilized pump line and the improvement in CEP stabilization electronics.

HERACLES is built upon an Optical Parametric Chirped Pulse Amplification (OPCPA) architecture. This architecture uses Optical Parametric Amplification (OPA) as the gain material to increase the output energy of the system. OPA relies on a nonlinear process to generate high gain (10^6) with ultra-wide bandwidth. Instabilities in the OPA driving pump energy can create dynamically fluctuations in the final OPCPA output energy. To reduce these fluctuations two key upgrades were implemented on the pump beam. Both were major improvements in the stability. Firstly, an improved regenerative amplifier design reduced beam pointing fluctuations. Secondly, the addition of a pump monitoring system with feedback-control eliminated long-term power drifts. Both enhanced the OPA pulse-to-pulse and long-term stability.

To improve the stability in measuring CEP drifts, modification of the feedback electronics was needed. The modification consisted of integrating noise reduction electronics. This novel noise reducer uses a similar process to a super-heterodyne receiver. The noise reducer resulted in 60 dB reduction of out-of-band noise. This led to increased signal quality with cleaner amplification of weaker signals. The enhanced signal quality led to more reliable long-term locking. The synthetically increased signal-to-noise ratio allows locking of the CEP frequency below the typically requirements. This integration allows relaxed constraints on the laser systems.

The optics and electronics of a high-power, quasi-single cycle laser facility were improved. This thesis included the stabilization of the pump line and the stabilization of the CEP. This work allows for new long-duration experiments.

TABLE OF CONTENTS

LIST OF FIGURES

LIST OF TABLES

LIST OF ACRONYMS/ ABBREVIATIONS

ADC	Analog to Digital Converter
AGC	Auto Gain Control
AIT	Above Ionization Threshold
AOFS	Acoustic Optic Frequency Shifter
AOM	Acousto-Optical Modulator
APD	Avalanche Photo Diode
ASE	Amplified Spontaneous Emission
BaF2	Barium Fluoride glass
BBO	Beta Barium Borate
BW	Bandwidth
CEP	Carrier Envelope Phase
CF	Center Frequency
CM	Chirped Mirror
CPA	Chirped-Pulse Amplification or Chirped-Pulse Amplifier
CW	Continuous Wave
DAC	Digital to Analog Converter
DDS	Direct Digital Syntheses
DOG	Double Optical Gating

FPGA	Field Programmable Gate Array
FWHM	Full Width Half Maximum
Grism	An optical pulse stretching device
HCF	Hollow Core Fiber
HeNe	Helium Neon
HERACLES	High-Energy, Repetition-rate Adjustable, Carrier-Locked-to-Envelope System
HHG	High Harmonic Generation
HR	Highly Reflective
HWP	Half Wave Plate
IF	Intermediate Frequency
IR	Infrared
LNA	Low Noise Amplifier
Nd	Neodymium
NOPA	Non-Collinear Optical Parametric Amplifier
OC	Output Coupler
OPA	Optical Parametric Amplification
OPCPA	Optical Parametric Chirped-Pulse Amplification
OPO	Optical Parametric Oscillator
Osc	Oscillator
PCF	Photonic Crystal Fiber
PD	Photo Diode

PID	Proportional–Integral–Derivative
Q	Quality
RF	Radio Frequency
SF	Super Fluorescence
SF57	A highly dispersive type of optical glass
SHG	Second Harmonic Generation
SPM	Self-Phase Modulation
SSG	Small Signal Gain
TFP	Thin-film Polarizer
VCO	Voltage Controlled Oscillator
VFO	Variable Frequency Oscillator
VGA	Variable Gain Amplifier
VIS	Visible
YAG	Yttrium Aluminum Garnet crystal
Yb	Ytterbium
YVO_4	Yttrium Orthovanadate crystal, “Vanadate”

1 INTRODUCTION

There are many applications of ultra-fast high-intensity laser pulses. These include High Harmonic Generation (HHG), attosecond pulse generation, THz emission, particles acceleration and filamentation. For many of these applications, a key element is the location of the electric field vector within the envelope of the laser pulse. The position of the peak electric field relative to the peak in the envelope of the pulse is called the Carrier Envelope Phase (CEP).

The first demonstration of controlled CEP was in 1996 [1]. Since then a large research effort has been undertaken to control the CEP in laser oscillators and amplifiers. In some experiments, the locking of the CEP to a specific value is desired. Locking the CEP requires measuring the phase drift within a laser pulse and applying a feedback for correction. The results show that with ultra-short laser pulses the CEP changes the interaction with materials. This is the case for both the formation of HHG [2] and the generation of terahertz emissions [3].

High intensity experiments have steered laser developers into two categories. The first approach is the traditional technology of Chirped-Pulse Amplification (CPA). In CPA systems, short pulse durations are created by spectral broadening techniques. A broadening technique used is Self-Phase Modulation (SPM) in a hollow core fiber [4]. The second approach involves the use of Optical Parametric Chirped Pulse Amplification (OPCPA) systems [5]. OPCPA systems rely on similar characteristics of CPA. The difference is the potential to directly generate a sub-four femtosecond laser pulses. OPCPA systems can amplify a super-broad bandwidth by Optical Parametric Amplification (OPA) [6]. Both techniques are moving to the shortest number

of cycles [7-9]. With either technique, as the pulse duration approaches quasi-single-cycle, the need for CEP stabilization becomes more prevalent.

This thesis focuses on the methods needed to stabilize the CEP in the HERACLES laser facility. It includes improvements in the HERACLES pump line for long-term stability. This not only improves the facility's performance, it also allows the measurement of slow CEP drifts. This thesis contributes to the body of knowledge of engineering of a stabilized OPCPA system. The following is the outline of this thesis and the challenges needed to engineer a stable OPCPA system.

Chapter 2 investigates the theoretical concept of a quasi-single-cycle pulse. It then branches to the concepts of CEP and the overview of OPCPA. The CEP section illustrates the need to control the electric phase difference as the pulse duration reduces. Methods in creating a high energy laser system are introduced through CPA and OPCPA schemes.

Chapter 3 gives the techniques needed to measure fast changing drifts of the CEP. This is observed in the output of mode-locked oscillators. The requirements of bandwidth and energy needed for the instruments are also discussed. Slow CEP drifts are created as the pulse travels through the system. Measuring and correcting these drifts is made possible through slow CEP locking techniques. The overview of the original technologies used in the HERACLES system is discussed. The new improvement in noise reduction allows enhanced performance to the original technology for fast CEP locking.

Chapter 4 provides an overview of the first generation of the HERACLES pumps. The issues of beam-pointing and long-term power fluctuation are discussed. Redesign of the pump line forms the second generation of HERACLES. This second generation improved output energies and with optimized feedback systems allows a long-term stable output.

Chapter 5 concludes the thesis with the HERACLES system containing a stabilized pump line and reduced noise electronics for CEP locking.

2 INVESTIGATION ON QUASI-SINGLE-CYCLE PULSES

The mathematical idea of an infinitely narrow optical pulse is not a new concept. This concept allows the simplification of complex properties of ultra-short laser systems. The model in the formation of ultra-short pulses will be discussed. Another simplification of ultra-short pulses is to represent the pulses as a frequency comb. Frequency combs become important in measuring the CEP. This chapter includes an outline of the CEP and how it affects the formation of sub-fs pulses. The impact in controlling the CEP as the pulse duration decreases is included. The techniques used to generate quasi-single-cycle pulses are provided. They consist of CPA and OPCPA schemes. Advantages in OPA characteristics that allow broadband amplification are discussed. This includes the requirements of a stable pump line to reduce the undesirable side products in an OPA architecture.

2.1 Conceptual Approach to a Single-Cycle Pulse

Any waveform can be constructed from a desecrate set of building blocks. In the mathematical explanation, a standard desecrate set of building blocks can consist of sine functions, each with a different frequency and phase. This was first described by Joseph Fourier in 1807 [10]. The unique wave that is represented as a combination of a series of infinite number of frequencies that all start propagating with the same phase at time zero is a delta function. The delta function has the value 1 at the origin and the value 0 at all other points. The process of constructive and destructive interference of sine waves can be used to describe the delta function.

To move a single delta function in different location in time, the phase of every sine wave has to be delayed. Thus, when every sine wave reaches a zero phase shift the delta function is generated. Equation (1) is the representation of temporally moving a delta function:

$$\delta(x-\alpha) = \frac{1}{2\pi}\int_{-\infty}^{\infty} cos[q(x-\alpha)]dq. \quad (1)$$

A periodic repetition of delta functions with a constant frequency separation could be represented as an infinite summation of phase shifted delta functions. A simplification of this infinite sum of delta functions allows dropping all sine terms that contains no multiple of the fundamental separation frequency. This series of unique frequencies is commonly referred to a frequency comb. Equation (2) represents this simplified series of an infinite set of delta functions that generates a frequency comb:

$$f(x) = a_0 + \sum_{n=1}^{\infty}(\cos(\omega n\mathrm{t})). \quad (2)$$

Frequency combs are nowadays a common tool for ultra-precise spectroscopy and optical atomic clocks. The combs with discrete frequency spacing are generated through the Fabry-Perot effect in a laser cavity. Fabry-Perot cavities allow only certain frequencies to oscillate. Further the amplification bandwidth of the laser system is limited. This restriction means that only a region of a frequency combs is effectively produced. In a laser system, this is referred to as selective gain. The limitation of selecting the number of desecrate comb frequencies transform the infinitely narrow pulses in time to broadened pulses in time. The change from a delta functions that consist of an infinitely narrow length of time to a specific length of time allows the introduction of pulses with single cycle carrier frequency. The cycle oscillation of the pulse is typically given by the center frequency (or wavelength) of the gain bandwidth. As the bandwidth

of the selective gain is reduce, the number of complete cycles of the fundamental wave increases. If only selects a single comb frequency is amplified the laser output would be a continuous wave (cw).

The following Equation (3) represents the relationship between a Gaussian bandwidth (FWHM) and its transform-limited pulse duration (FWHM), where λ_0 is the center wavelength and τ is the duration of the pulse (FWHM):

$$\Delta\lambda = \frac{2ln2{\lambda_0}^2}{\pi c\tau}. \quad (3)$$

An interesting problem that occurs for ultra-short optical pulse trains is the addition of a phase difference between consecutive pulses. If this phase is not equal to zero, the electric field of consecutive pulses will have carrier waves not crossing the zero point at the same location. Therefore the total envelope that defines the shape of the pulse changes location in respect to the central frequency. This offset is referred to as Carrier Envelope Phase (CEP). Figure 1 represents the phase differences between the envelope and the electric field.

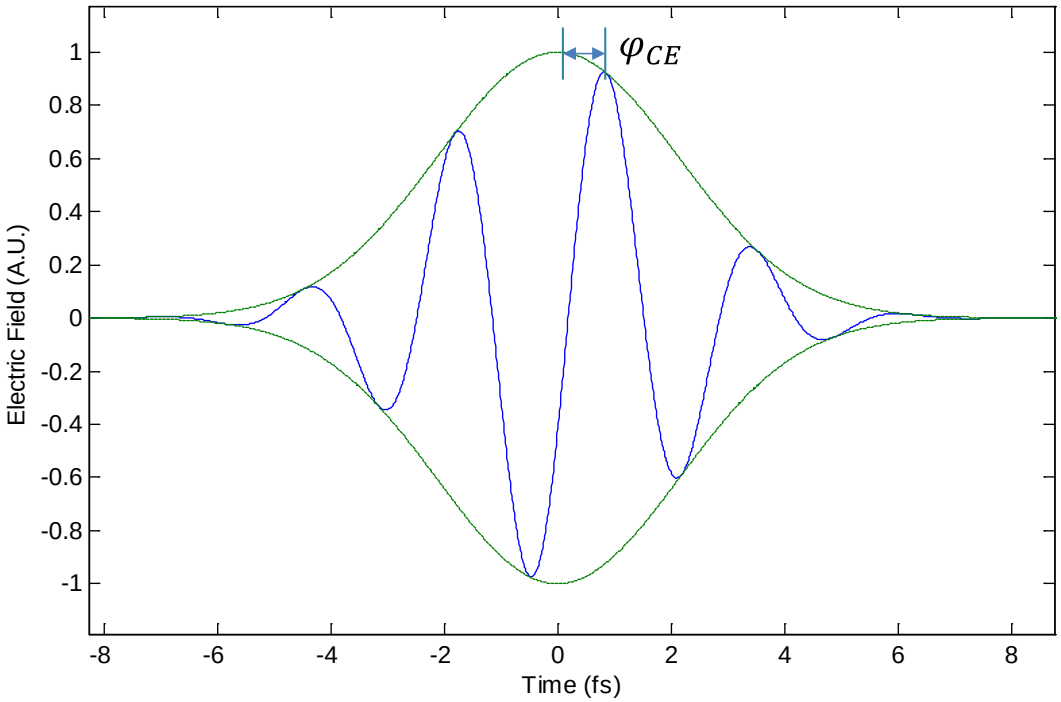

Figure 1: Difference in the group velocity and phase velocity generating the CEP of a normalized 5 fs Gaussian pulse.

2.2 Basic description of the Carrier Envelope Phase

The first demonstration of absolute control of a frequency comb was for use in ultra-precise spectroscopy [11]. The ability to tune the combs to allow precise measurements greater than the hyperfine structures of atoms was possible and gave experimentalist the ability to probe a sample with a nearly exact frequency (accuracy of 10^{-16} in 1s [12]). This was first demonstrated by Roy Glauber, John (Jan) Hall and Theodor Hänsch in 2000 and were rewarded with a joint Nobel Prize in 2005 [13].

The ability to tune the comb allows the sweeping of the spectrum giving a near constant probe spectrum. In 1999 it was proposed that for quasi-single-cycle pulses the electric field

underneath the envelope would play a large role in highly nonlinear experiments, primarily driven by HHG [14]. Generating isolated attosecond pulses can be made possible by decreasing the pulse duration of the femtosecond pulse to perform sub-cycle gating via the short pulse duration. This sub-cycle gating via quasi-single cycle pulse duration is the approach followed in our laser system and will be explained in the following paragraphs. The second successfully proven method to generate isolated attosecond pulses is double optical gating (DOG) [15]. It has been used to generate the currently shortest pulse duration achieved with 67 as [16]. This process works by using two optical techniques that hinders the generation of attosecond pulses at different locations. One of the optical techniques used to form the DOG is polarization gating. The Above Ionization Threshold (AIT) is dependent on the polarization of the incident beam. It is found that for elliptically polarized light the AIT is higher than for linearly polarized light. To perform polarization gating the beam is shaped to be elliptically polarized until the pulse is at the maximum, to where the beam becomes linearly polarized and then is transformed back to elliptically polarized [17, 18]. The second technique used in DOG is two-color gating. In two-color gating a probe beam is used to destructively interfere with the pump beam. This then only allows HHG to generate an attosecond pulse every other half cycle. With both techniques combined one has the ability to isolate a single attosecond pulse.

In sub-cycle gating via quasi-single-cycle pulse duration the peak electric field is higher than the ATI and all other peak electric field strengths are below the threshold [19]. This is primarily controlled by the pulse duration and the CEP of the pulse. The generation of an attosecond pulse appears near the zero point of each electric field oscillation. With the decrease of the temporal pulse width, the number of generated attosecond pulses decrease until one to two pulses are left. The scheme is shown in Figure 2.

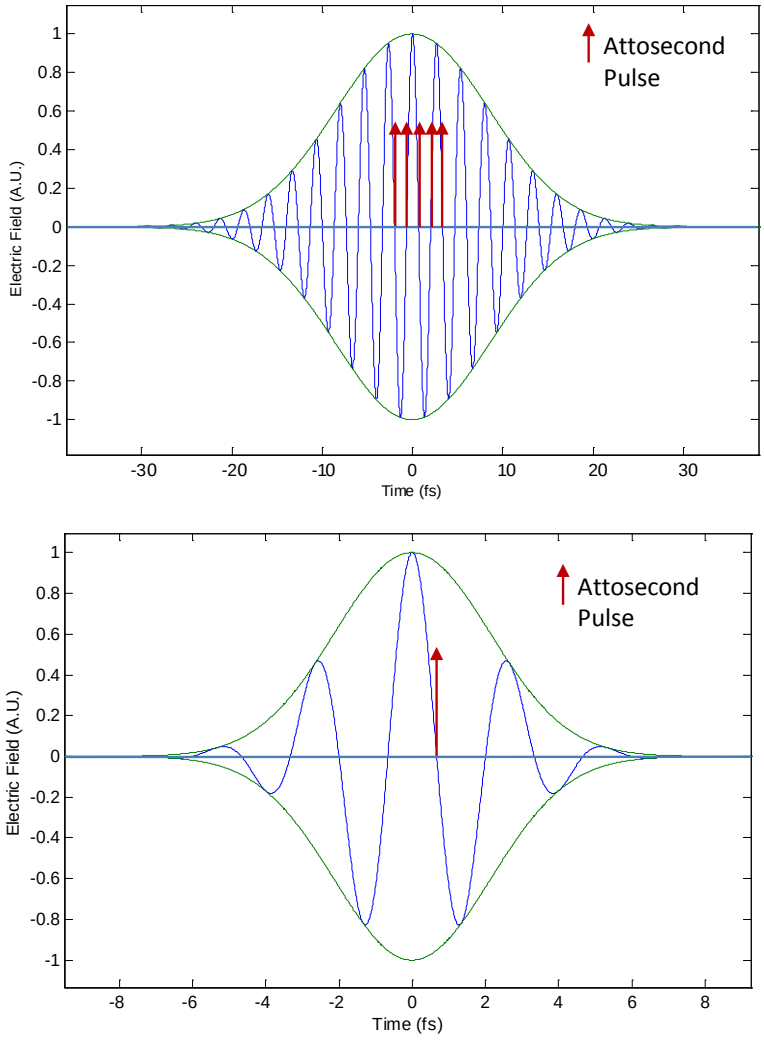

Figure 2: Top: Simulation of Sub-cycle gating, where the pulse generated 5 attosecond pulses when having a 20 fs (FWHM) pulse duration. Bottom: A 5fs pulse generates an isolated attosecond pulse in the chosen configuration.

If the CEP of the laser pulse is not controlled to a fraction of π the continuous drift of the phase relationship between the electric filed and the envelope ϕ_{CE} could produce multiple attosecond pulses. Usually with lower energies and emitted at different reference points in time. Figure 3 shows the influences in the location of the electric field has to produce a single pulse or a double pulse of attosecond light.

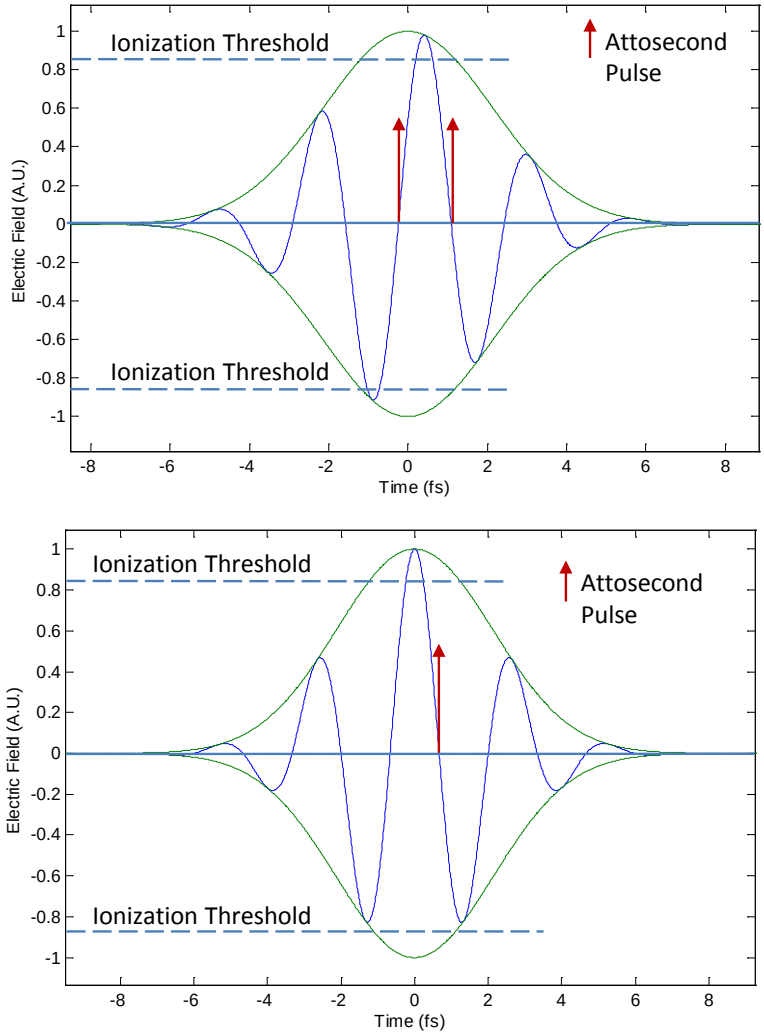

Figure 3: Without control of the CEP the point in time when the attosecond pulse is generated and its energy become randomized for 5 fs pulse duration. The threshold is arbitrarily chosen to provide an overview of the impact.

In addition to the possibility of generating a varying number of attosecond pulses without control of the CEP, another issue occurs when the pulse duration decreases. If the experiment required the CEP phase difference to be exactly Ω rads, the pulse duration would control the electric field strength by Equation (4):

$$E(\Omega) = e^{\frac{-2ln(2)\left[\frac{4\Omega}{3\pi}\right]^2}{t_{FWHM}{}^2}} . \quad (4)$$

With the continuous decrease in pulse duration, the electric field would dramatically change if only a small fraction of CEP drift occurs. Figure 4 is the calculated normalized electric field strength of different pulse durations at different CEP phase locations.

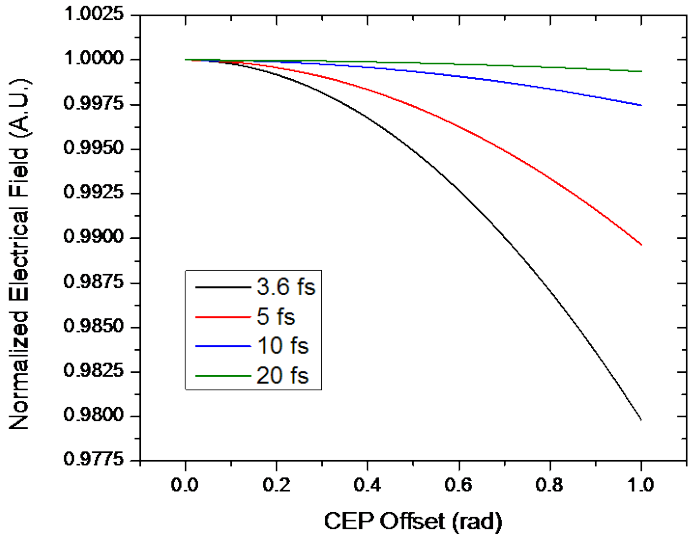

Figure 4: Electric field dependence on pulse duration given by Equation (4).

If the experiment was done with a laser output of around 20 fs (9 cycles) the output difference of a 100 mrad phase change would translate in an electric field strength change of less than a ratio $1{:}10^7$. If the same task was carried out for a 3.6 fs laser pulse (sub-2-cycles) the electric field strength would change by 1:5000. These fluctuations are reduced when locked to the zero point, but if the same scenario was chosen and the offset was set at 750 mrad, then the change in the 20 fs would be $1{:}\ 10^4$ and for the 3.6 fs would be 1:300. With an even higher offset, this produces inconsistent measurements and could obscure the experimental results.

Experimentally controlling the CEP demonstrated the high dependence of the electrical field and the envelope with the generation of HHG, this leads to higher and stable conversion efficiency compared to non-locked systems. In 2004, a sub-5-fs laser system with controlled CEP of $\pi/4$ generated a single attosecond pulse [2]. The emission of less intense attosecond pulses could not be avoided due to the given pulse duration, however, a band pass filter only allowed the attosecond pulse generated with the pulse with highest electric field strength to transmit. The group was able to demonstrate (i.e. generate and characterize) a current world record 67 as pulse using similar techniques [16].

2.3 CEP Control

In ultrafast laser systems the CEP can drift as it propagates through the optical components in the system. The characteristic that allows change of the CEP is when the group delay and group dispersion are not matched. Two elements that change the CEP and allow small controllable changes of the CEP in the system are the compressor and the stretcher [20, 21]. Assuming that the incoming beam enters a stretcher with a linearly polarized field, then as the pulse propagates through a grating the spectral phase is described by Equation 5. Where P' is the optical path length, G is the perpendicular distance between gratings, d is the grating constant and B is the diffraction angle:

$$\varphi(\omega) = -\frac{\omega}{c}\mathrm{P}'(\omega) + 2\pi\frac{G}{d}\tan[\beta(\omega)]. \quad (5)$$

The CEP shift is then derived by the difference between the group delay and the phase delay. Equation (6) shows that the separation of the gratings or the diffraction angle changes the CEP through the stretcher:

$$\Delta\varphi_{CE} = 2\pi\frac{\Delta G}{d}\tan[\beta(\omega)], \quad (6)$$

where, ΔG is the path change that could be introduced through vibrational fluctuations and drifting.

If only the separation of the grating is used to calculate the phase shift and the assumption of the tangent term drop close to 1 with angles greater than 45 degrees. Then with the increase in grating density the difference in separation between the gratings will increase the phase shift. If the density of the grating was on the order of 300 lines per mm then a change of 1.6 μm of drift would represent a π shift. If the grating ruling was 1200 lines per mm then the π change would occur in ~420 nm. This implies that stretchers with high groove density gratings have higher CEP drift noise compared to systems with lower line densities.

Another technique used to stretch a pulse is a Grism stretcher. A Grism is a design that contains both a grating and a prism. The advantage of this design is the ability to tailor the added third and fourth order dispersion to match the dispersion of a bulk material. This allows the final compression through a bulk material. The exact control of the third and fourth order dispersion is through the geometry and material selection of the prism.

In the case of a grism, the exact calculation of the change in CEP with changing the separation is more complex compared to the stretcher Equation (6) given above. A computer simulation was used during the initial design of the grism dispersion. It is possible to calculate the CEP changes from this simulation code.

2.4 OPCPA Overview

The generation of quasi-single-cycle pulses with ultra-high intensity is based on two methods – CPA [22] and OPCPA [23]. The CPA technique relies on the process of building a high peak power laser system with limited bandwidth commonly referred to as CPA (Chirped Pulse Amplified) laser system. At the end of a CPA laser system the bandwidth can be spectrally broadened by generating a super-continuum in a hollow core fiber (HCF) to achieve a sub-10-fs pulse duration [4]. The major drawback for this approach is the maximum amount of energy that can be handled by the HCF and the dispersion management. Without the correct dispersion management, the compression of the pulse is not possible. The OPCPA method that was proposed in [23, 24], is similar to CPA in that it relies on stretching, amplifying and compression of the pulse. A key difference is that in OPCPA the ultra-broadband bandwidth is preserved through amplification since effectively no gain narrowing occurs [25, 26]. To date, OPCPA have demonstrated scalability for high pulse energy as well as high average power. Meanwhile most high-intensity Ti:sapphire-based CPA systems operate at the 10 W average power level due to thermally induced beam distortions in the amplifier chain. These distortions are imprinted directly onto the signal beam. With new technologies of cryo-amplifiers, CPA systems are breaking through these limitations. In OPCPA, the seed pulse only passes through a stretcher, OPA and compressor. This relative short optical path and the reduction in thermally introduced beam distortions since the OPA has no associated energy storage and therefore no quantum defect heating. However, the requirements on the pump beam are a significant challenge in OPCPA. Due to the nature of the nonlinear amplification in the OPA, the OPCPA output is nonlinearly dependent on the quality and stability of the pump beam. Thus, a high quality pump

beam must have low pulse-to-pulse fluctuations, low long-term power drifts, well behaved Gaussian or top-hat beam profile, low timing jitter and stable beam pointing.

2.4.1 OPA Theory

Optical Parametric Amplification (OPA) relies on the $\chi^{(2)}$ properties of an optical nonlinear medium. For the Ti:sapphire wavelength at 800 nm the material of choice is commonly BBO [27]. As the seed and the pump beam pass through the material, energy is transferred from the pump to the seed pulse and the seed pulse is amplified. Due to the conservation of momentum and energy, this process also generates an idler beam with the photon energy equal to the difference between the seed and the pump energies [28]. The following Equations (7) and (8) represent this, where k_p, k_s, k_i are the wave vectors of the pump, signal and idler and $\omega_{p,s,i}$ are the corresponding angular frequencies

$$\hbar k_p = \hbar k_s = \hbar k_i, \tag{7}$$

$$\hbar \omega_p = \hbar \omega_s + \hbar \omega_i. \tag{8}$$

For an 800 nm seed and a 532 nm pump the idler wavelength is 1588 nm. The idea of phase matching for multiple frequencies allows multiple frequencies to be amplified. This is done by selecting the “magic” angle between the incoming signal and pump beams as well as the angle with respect to the orientation of the nonlinear crystal [29]. Figure 5 consist of simulated matching conditions of a BBO crystal being pumped by 532 nm light.

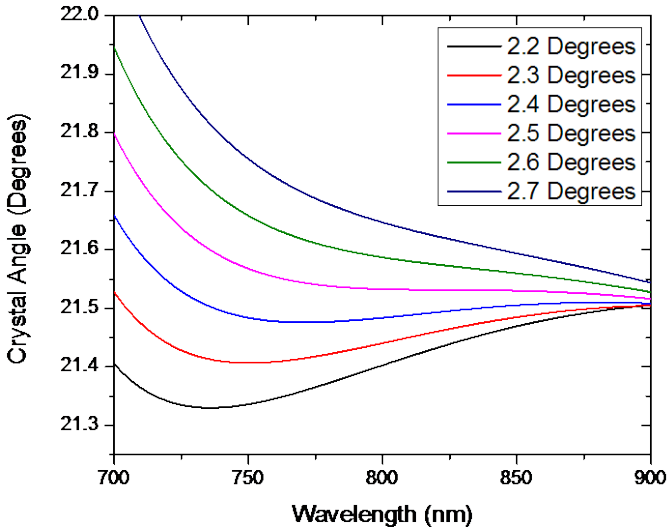

Figure 5: Phase matching curves showing the tuning angle vs. crystal angle simulated through the software package SNLO.

When the signal and pump beam propagate collinearly, this is referred to as degeneracy. This case is commonly used in narrow bandwidth, tunable sources or Optical Parametric Oscillators (OPOs). An OPO is seeded by super fluorescence (SF), produced through a random quantum-mechanical process. These lasers are commonly referred to as tunable laser sources, due to the ability to tune the phase matching condition through a wide range of spectra.

2.4.2 Parasitic Processes in OPA

The difference between an OPO and an OPA is that the seed is created by a random process in an OPO whereas an OPA is seeded from an external source. In general, OPA and SF are competing processes [30, 31]. If the seed amplitude becomes too weak, the amount of generated SF will increase. Amplified SF in consecutive OPA stages is an issue with OPCPA laser systems since it generates an uncompressible section of the pulse. A similarity can be seen

to CPA systems, which produce Amplified Spontaneous Emissions (ASE) during amplification resulting in uncompressible background.

The non-collinear OPA (NOPA) architecture has specific tuning angle, the termed “magic angle”, that allows for the broadest parametric gain bandwidth. The gain bandwidth dramatically reduces if the angle between seed and pump deviates slightly off from this angle.

2.4.3 OPCPA Stability with Real Beams

In the process of nonlinear amplification the power and energy fluctuation of the pump beam has great influence on the parametric gain. The critical properties that determine the parametric gain of the system are the photon energy, the pulse intensity of the pump, the angle between seed and pump relative to the angle to the optical axis of the crystal. Since common laser systems show limited stability. Both in the pointing and in the output power, the parametric gain in nonlinear medium can change dramatically. Changes in beam pointing of a system will not only influence the gain bandwidth due to angle detuning, but also the spatial overlap of the seed and the pump. If only a fraction of the seed and pump are spatially overlapped the effective parametric gain for the seed will be dramatically reduced and the generation of super fluorescence will increase. The quality of the pump beam used for an OPA system can dramatically change the output of an OPCPA laser system, both in bandwidth (pulse duration) and output power.

2.5 Summary

The concepts of frequency combs and the formation of ultra-short pulses are presented. CPA and OPCPA techniques used to create a high energy laser system were also introduced.

Finally, an overview of the OPA characteristics, this includes broadband gain and the pump requirements necessary for reducing SF.

3 CEP CONTROL SYSTEM

The ability to measure and control the CEP of an OPCPA laser system relies on two feedback systems. The first measures the constant phase change in the oscillator and locks it to a reference source, usually the oscillator's repetition rate. The second measures the slow CEP drift that naturally occurs throughout the system and feeding back to the oscillator to compensate this drift. Both of these measures, as well as standard operation parameters (temperature management, mechanical stabilization, pump power, etc.), must be managed and optimized by an "integrated" control systems to ensure stable locking of the laser facility.

3.1 Techniques to Measuring Fast CEP

A direct measurement of the CEP from an oscillator is difficult due to the low electric field strength and fast drifting [32]. A promising alternative has been presented by detecting the drift rate of the CEP [33]. The common way to lock the oscillator's CEP is by locking the drift rate to a constant reference source. This drift rate is referred to as CEP beat frequency. The best reference source in the laboratory is the highly stable laser repetition rate, typically on the order of 85 MHz given by the oscillator resonator cavity. The system usually locks to one fourth of the repetition rate.

The device used to lock the CEP beat frequency relies on a similar process of RF mixing. The mixed output is the sum and difference between the CEP and the f_{rep}. As the CEP beat frequency approaches to half the repetition rate, the signals become closer and closer together.

Until the CEP beat is exactly half the repetition rate and the two signals overlap on top of each other, producing a double image.

This double image makes locking challenging. Its effects can be avoided by locking to ¼ of the repetition rate. Figure 6 is when the CEP beat approaches half the repetition.

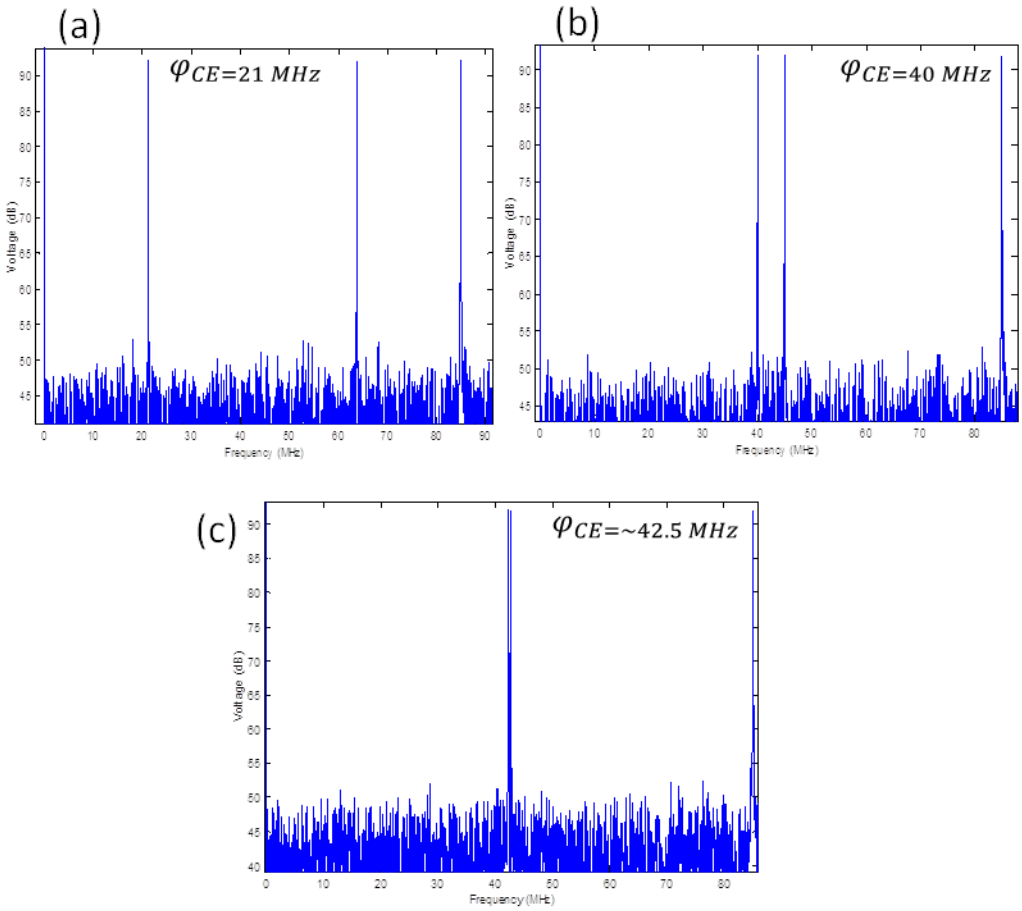

Figure 6: CEP beat note approaches half the repetition rate the folded signal begins to overlap with the non-folded signal. (a) Beat note at 21 MHz and a separation of 43 MHz. (b) Beat note at 40 MHz and a separation of 5 MHz. (c) Beat note at 42.49 MHz and a separation of 20 kHz.

As a consequence of locking the changing CEP beat to one-fourth the repetition rate, every fifth pulse in the laser output pulse train has the same CEP phase. Figure 7 illustrates that

every fifth pulse has the same relationship between the pulse envelope and phase with a constant phase shift of one-fourth the repetition rate.

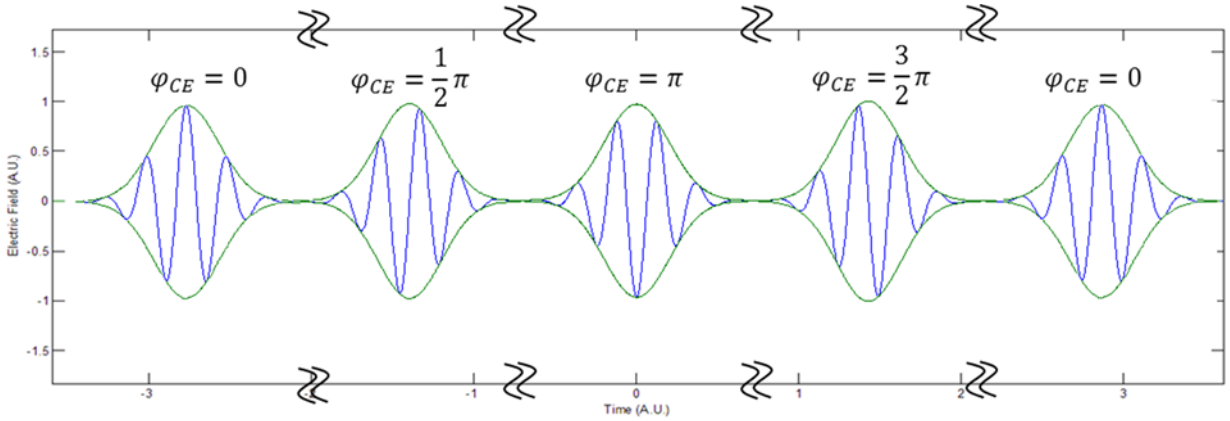

Figure 7: CEP beat with a change rate of $f_{rep}/4$. The pattern repeats after 4 pulses in the pulse train.

Since most laser systems reduce the laser repetition rate when amplifying, locking of every pulse is technically not needed. The repetition rate can be reduced such that all the pulses to be amplified will have the same CEP phase. This method enables fully CEP-stabilized over several kHz to MHz repetition rate when utilizing CEP-feedback.

3.2 Octave Spanning Frequency Comb

To generate the beat note used to lock the fast drifting CEP, an f-to-2f interferometer is used. The basic design requires a broadband source with a bandwidth ranging larger than one octave. The red side of the spectrum (1140 nm) is frequency doubled (to 540 nm) and further mixed with the fundamental frequency of a blue section of the spectrum (at 540 nm). This generates a temporal interference pattern on a fast (avalanche) photo diode. The frequency components are represented in Equation (9), where f_{ceo} is the CEP beat offset frequency:

$$f(x) = a_0 + \sum_{n=0}^{\infty}\left(a_n n \cdot f_{rep} \pm b_n f_{ceo}\right). \quad (9)$$

The resulting wave form that represents the CEP phase change can be extracted from the waveform and used to lock the laser. Figure 8 shows the calculated temporal output of the implemented f-to-2f interferometer.

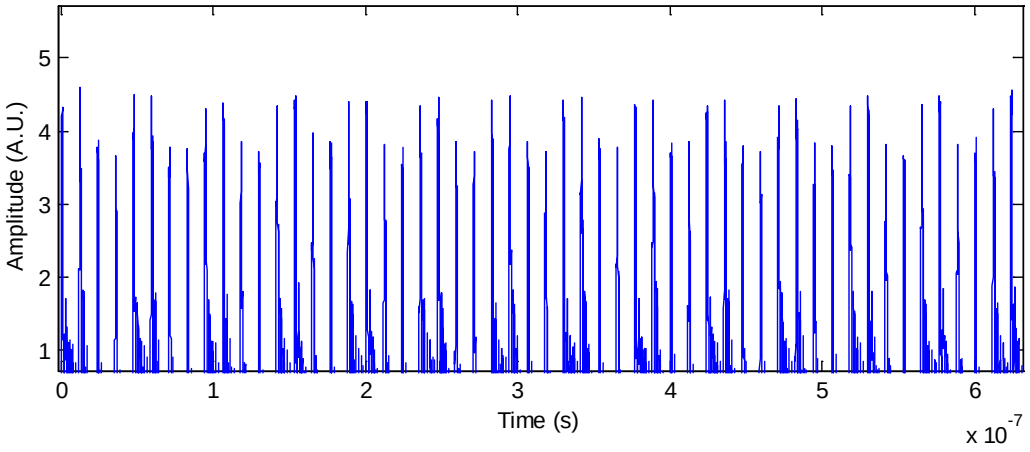

Figure 8: Calculated temporal output of an f-to-2f interferometer.

Two techniques are used to generate an octave spanning source needed for the f-to-2f interferometer. This octave spanning spectrum can be generated directly within a mode-locked oscillator, as in the HERACLES system. This requires that the dispersion within the oscillator be exactly compensated in order to drive the oscillator in the highest nonlinear regime possible to achieve the high intensity necessary to generate octave-spanning bandwidth. With such high intensity inside the crystal, damage initiated primarily by multi-photon ionization is a significant concern that can impact the reliability of the laser system.

Alternatively a separate nonlinear material can be used so that the octave-spanning spectrum is generated externally of the oscillator. A common device used for spectral broadening is highly nonlinear photonic crystal fiber (PCF) [34, 35]. When the oscillator beam is launched

into the fiber, self-phase modulation (SPM) broadens the spectrum. Equation (10) shows how the intensity of the oscillator changes the output of the spectrum [36]:

$$\Delta\omega = \frac{2\pi}{\lambda} n_2 L \frac{d}{dt} I(t) \, . \tag{10}$$

A drawback of this method is that any variation of the laser intensity $I(t)$ will introduce spectral modulation onto the broadened signal as seen in Equation (10). The added modulation can trick the feedback system used to lock the CEP rate of the oscillator.

Once an octave-spanning spectrum is created, the next step is then to mix the visible light with the frequency doubled from the IR spectrum. Since the generated light has extremely short pulse duration, the two pulses must overlap well in space and time. Figure 9 shows the basic scheme used in this thesis. First, the system is built collinearly where both beams propagate along a common optical axis so that spatial overlap is inherent. Second, the temporal overlap can be engineered with dispersive elements. The dispersion introduced by any elements through which the pulses propagate. These elements are the output coupler of the oscillator, the beam splitter and the focusing lenses, are generally positive dispersive and move the IR and VIS further apart in time. Chirped mirrors can be used to introduce the negative dispersion necessary to compensate for this positive dispersion and will allow fine adjustments made by the insertion of a pair ofBaF_2 wedges.

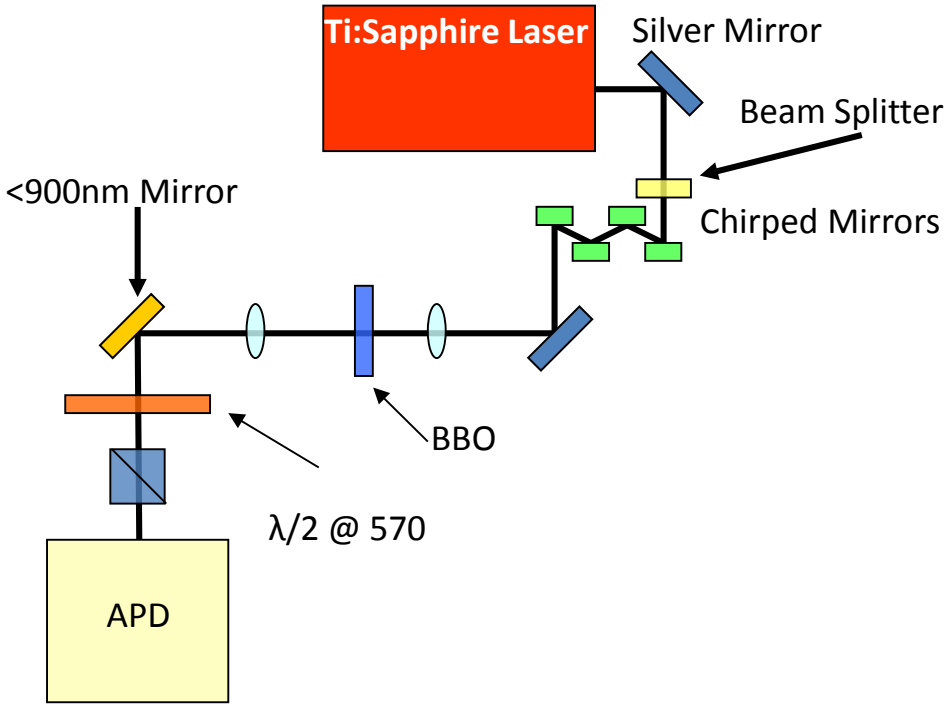

Figure 9: Scheme of a collinear f-to-2f interferometer.

Another method to ensure spatial and temporal overlap is the use of a Michelson interferometer-like setup as shown in Figure 10. In the interferometer system, half of the beam is split with a duplexing mirror, which is a dichroic mirror reflecting the lower frequencies and transmitting the higher frequencies. The second harmonic crystal is placed in the IR arm of the interferometer to frequency double the IR to the visible spectrum. An additional delay line allows temporal overlap adjustment. Half-wave plates can also be added to increase the polarization overlap. The final step is to then recombine the two arms and measure the beat generated by the interference of the two arms.

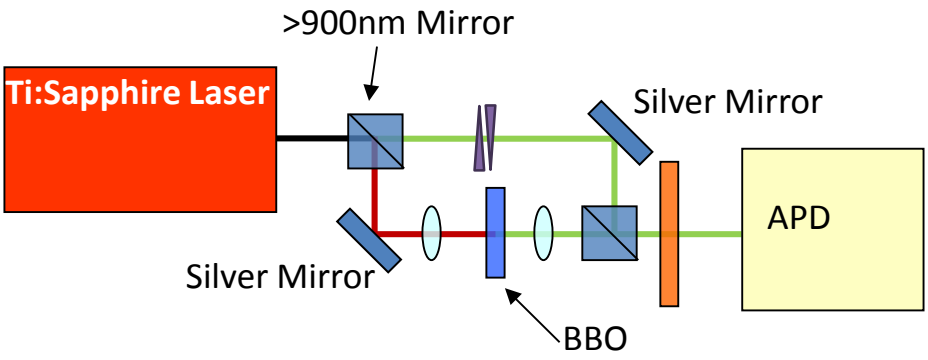

Figure 10: F-to-2f interferometer based on a two arm Michelson interferometer.

A drawback of the Michelson interferometer scheme is additional noise introduced into by using two arms. Vibration of the mirrors modulations the signal and leads to additional phase noise in the feedback system. A technique used to compensate vibrational fluctuations between the arms uses a reference source. The technique locks the length of both arms with respect to each other. A HeNe laser can be used as a reference and a piezo mirror with a feedback loop allows for stabilization [37]. It has been shown in [38] that this approach can increase the stability of the CEP measurements by two orders of magnitude.

3.3 CEP Locking Technique

The largest supplier of locking systems used by nearly every research facility to lock the CEP is by MenloSystems GmbH. Their design consists of a pre-amplifier, a frequency divider, a phase error detector and a feedback loop filter. The output from the loop filter is taken through an RF driver that is used to modulate the pump beam of the Ti:sapphire oscillator via an AOM. The process works by slightly temperature-tuning the refractive index of the Ti:sapphire crystal which further slightly changes the optical path length of the oscillator and effectively moves the CEP. This process allows the fast locking of the CEP with minimal resonator distortion. The

large modulation bandwidth of the AOM allows potential sub-MHz changes to the locking scheme. The limiting element is the loop filter bandwidth is on the order of a few hundred kHz. The total locking lifetime is limited to the maximum modulation amplitude that the AOM can perform without making the laser cavity unstable. Typically, locking can be achieved for several hours during an experiment [39] without additional feedback mechanisms.

The CEP usually drifts with a slow, almost constant rate. At some point in time the output of the loop filter will approach the maximum safe output and the system will drop phase-locking. One method that is used to compensate for this limitation is with the addition of temperature tuning to the laser cavity. The concept of this scheme is to detect when the loop filter is approaching the 70 % of the maximum allowable DC offset and then starts to apply a temperature change to the TEC controller used to stabilize the Ti:sapphire crystal temperature [40]. This process also is commonly used to stop the slow drifting of the CEP in the slow f-to-2f CEP measurements. This process then allows the ability to lock the CEP of the laser from a few hours without the feedback scheme to days with the feedback scheme.

A layout sketch of the CEP phase locking electronics is shown in Figure 11. The stability of locking the CEP of the system is primarily determined by the signal to noise ratio of the modulated input from the avalanche photo diode. The Menlo-Systems phase-locking electronics takes the input from the APD and passes the signal through an 18-24 MHz band pass filter. The filtered signal should only contain the CEP beat note. It is subsequently passed through a high gain amplifier circuit with a gain of 60 dB. The signal is further sent through a secondary amplifier to be used as an output reference where a RF spectrum analyzer determines if the CEP beat tone has proper location and signal to noise ratio. The phase detector used in this system, consists of Schmitt triggers to square up the analog signal and the signal form the divider circuit.

The modified (squared) waveforms are passed to a Field Programmable Gate array (FPGA) to compare the phase difference between the two. If the FPGA determines that the rising edge from the APD waveform was acquired before the reference signal, a counter is incremented. If the reference signal arrives before the APD then the counter is decremented. The output from the eight bit counter is then applied to a resistor network that uses the digital output form the FPGA to form an analog output. The resolution of the digital to analog converter then allows step sizes of 18 mV. This design also generates a high amount of error since the counter will always change with every pulse input. If both signals are arriving at the same time and no corrections are needed, the device will still change its output. Another issue of the design is that if the phase difference is somewhat unstable in the way that the phase difference between CEP beat and the reference changes rapidly. The phase locking electronics will not be able to adapt to this and could possibly not generate a stable phase lock.

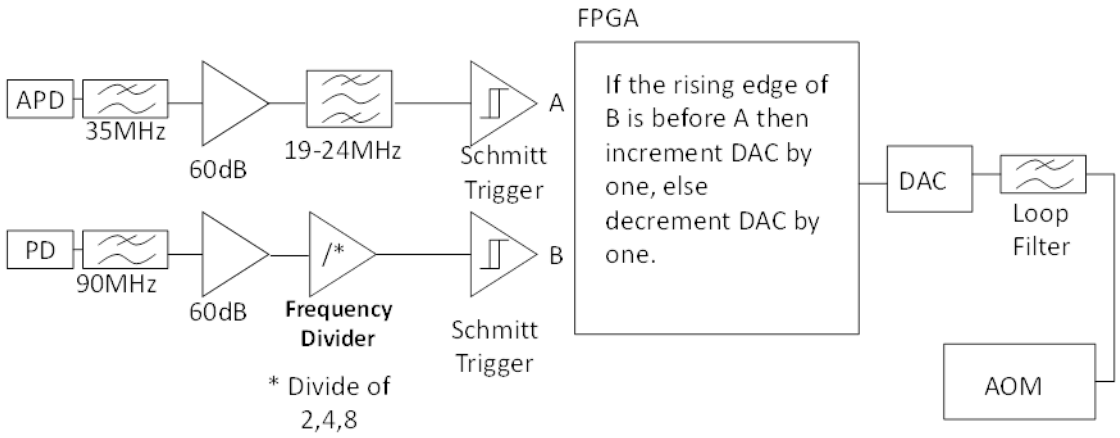

Figure 11: Block diagram of the Menlo CEP locking system.

As the signal to noise ratio decreases from the CEP signal, the Schmitt triggers are used to generate the signals needed for the FPGA become more susceptible to the out-of-band noise floor. The typically lowest S/N ratio to correctly lock the CEP beat note is at least 30 dBc. This

limitation requires the oscillator to be able to generate enough IR power to create this signal. The 1140 nm light portion needed to generate this output is at least 30 μW. This is measured with a narrow band-pass filter (Thorlabs FB1150-10). This necessary power brings the oscillator close to the surface damage threshold of the crystal. This point of operation demands no other modulation on the output of the laser. It requires delicate adjustments to properly align the oscillator to the correct region of stability.

Another scheme to lock the CEP is termed zero-CEP-offset-locking [41-43]. The process of zero locking enables every pulse of the MHz oscillator output to heave the exact same phase. This then reduces the need for a pulse picker to remove all pulses that does not contain the same phase. It also allows the laser system the ability to maintain the high MHz repetition rate. The technique used to accomplish zero phase locking is through the use of an optical frequency shifter. The shifter generates an offset that is used to produce the signals needed for the feedback system. The system needs to have a difference in the fringe frequencies between the visible and the IR. If the same f-to-2f interferometer that is used in the constant CEP beat is used to zero lock the signal. The beat would coincide with the repetition rate signal making it impossible to lock. This is a similar condition that occurs when locking at half of the repetition rate. If a non-collinear design is used for the interferometer a frequency shifter can be used to move one of the frequencies up in frequency to be a given amount. An example of this design is that if the oscillator had a repetition rate of 20 MHz then the Acoustic-Optic Frequency Shifter (AOFS) shifts one of the arms to a frequency with a range of 3- 7 MHz. This then adds an offset frequency that when the mixing of the difference in frequencies of the two arms then produces a beat with the same frequency as the modulation frequency plus the CEP frequency. If the CEP frequency beat is at zero. Then the output is exactly the same frequency as the driving frequency

of the modulator (3- 7 MHz). The locking electronics then use the modulator's driving frequency as the reference to allow phase locking.

3.4 Techniques to Measuring Slow CEP

At the end of the laser system, the final output needs to be characterized to allow for the optimum operation on experiments that are affected by the CEP. At the beginning of the system the CEP of the oscillator is locked to a constant changing in rate. Due to slow mechanical and thermal drifts in the stretcher and through other elements in the system, the CEP of the pulse drifts as it propagates. If the CEP was measured at the end of the line, a feedback system could correct for these slow drifts.

MenloSystem has built an all-in-one system that performs the task of measuring the slow CEP drifts for a CPA/OPCPA system (APS800). The system requirements are 10 μJ of input energy and at least 50 fs of pulse duration. For reliable measurements the pulse-to-pulse jitter needs to be less than 1%. This is a changing requirement in the first generation of the HERACLES system.

The process in measuring the slow CEP drifts through the Menlo system is similar to the collinear f-to-2f system used to measure the fast CEP beat. The key difference in this design is to generate a broadened spectrum that occupies over one octave. To produce the octave spectrum, this system generates a single filament through a plate of Sapphire. The resulting supper continuum output is then recollected and passed through a doubling crystal. The second harmonics that the doubling crystal produced overlaps with the original spectra from the continuum and produces spectral fringes. With the implementation of the fast CEP locking system for the oscillator, the drifting of the CEP should be on the order of milliseconds. This

then makes it possible to track the spectral fringes using a spectrometer, which would have not been possible without the use of the fast CEP locking. A software package included with the system performs the required operations to measure the drifting of the CEP and output to a National Instruments DAC card to feedback into the oscillator to correct the slow drifting of the system.

3.5 CEP Stabilization on HERACLES

The initial design for the fast CEP feedback system used the MenloSystems control unit. A requirement for this system is the high IR output power necessary to successfully lock the CEP beat of 30 μW measured after transmission through a narrow band pass filter (Thorlabs FB1150-10). To reduce the requirements on high IR power, coupling optics of the f-to-2f interferometer were optimized in order to improve the collected the beat frequency and signal of the avalanche photo diode.

An interesting issue occurs if the APD is operated in saturation. In this case, the APD generates a secondary beat tone that could show up in the analyzed frequency spectrum. A characteristic of this beat tone frequency f_d is its frequency change when adjusting the APD gain. Small pulse energy fluctuations also translate into a frequency shift. In some initial experiments with HERACLES, this tone f_d was used to lock the system. Figure 12 shows a set of data collected from a case with an unlocked tone and a locked tone of the incorrect CEP beat note. The locked case of this system showed that even with tone f_d used as reference tone instead of the correct CEP beat tone, the phase-locking mechanism works. Other modulations of the system could introduce misleading tones and prevent the locking of the correct CEP beat tone. The following graphs also show that the locking electronics used for locking this beat tone

f_d could not lock the beat perfectly and the feedback loop filter used had limitations to fast changing tone jitter.

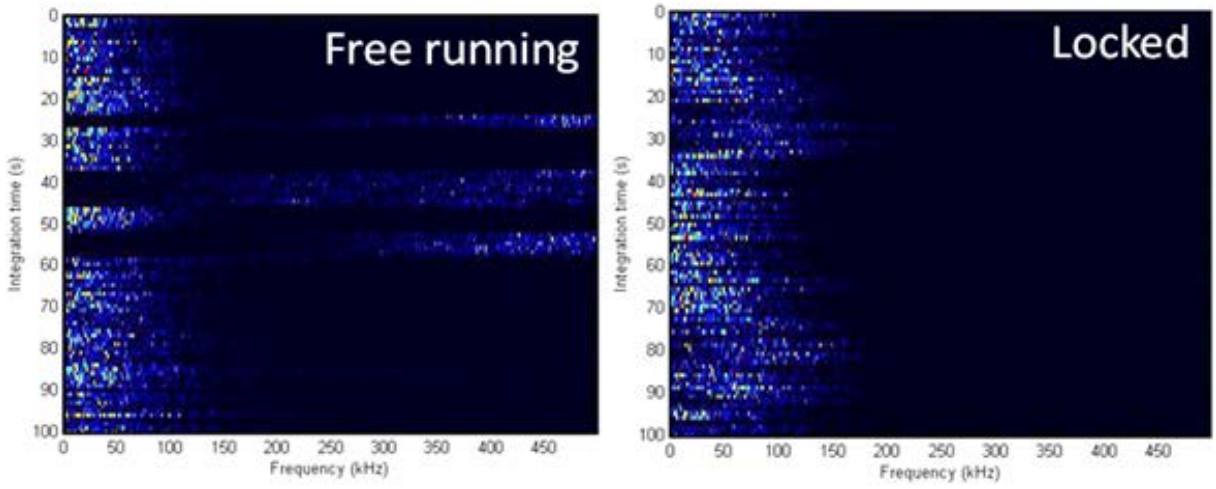

Figure 12: Left: A waterfall of the saturated APD. Right: Attempt to lock to the saturated APD as the CEP beat frequency.

3.6 Methods that Improves the Fast CEP Loop System

One of the key requirements in generating the fast CEP beat note is the f-to-2f interferometer. The temporal overlap of the IR and VIS needs to be optimized in order to allow the highest visibility possible. The first generation of the HERACLES system relied on a collinear f-to-2f interferometer. This design allows the highest stability since no noise is added by the optical components compared to the two arm interferometer designs. In order to optimize the temporal overlap the calculation of all dispersive materials must be used to allow the maximum overlap of the two. In the HERACLES system the only elements through which the pulse propagates are the output coupler, the frequency selective filter, the path through air and the focusing lens. To compensate for these positive dispersive materials a negative dispersive material must be used to allow the correct amount of dispersive overlap. Table 1 shows the delay

between 570nm and 1140nm for the elements in the path between the oscillator and the BBO crystal in the f-to-2f interferometer.

Table 1: Dispersion calculations for elements between the oscillator and the f-to-2f interferometer.

Object	Material	Thickness	Total GD
Output Coupler	FS	2 mm	125 fs
Beam Splitter	FS	2 mm	125 fs
Path Length	Air	151 cm	55 fs
Lens	CaF_2	4.32 mm	210 fs
Chirped Mirrors (CM)	--	--	-510 fs
		TOTAL	5 fs

The negative dispersive element that is used to compensate this dispersion is chirped mirrors. These mirrors work with the help of multi-film layers of specific thicknesses. These layers reflect wavelengths at different depths through the multi-layer stack when the Bragg condition is met. Depending on the design of the film structure thickness and refractive index a small amount of customized dispersion can be created. The amount of chirp generated through these mirrors is set and cannot be changed once manufactured. It limits the ability to control the dispersion if the design is changed or if additional adjustments must be made afterwards. To allow some fine tuning of the dispersion the use of a pair of glass wedges are used. This allows the ability to slide a wedge into the beam-path changing the dispersive properties and preventing the beam from walking off. The design to allow small adjustments to the dispersive elements in the f-to-2f interferometer was not introduced in the first generation of CEP measurements. The benefits of these adjustments are greatly impact the ability to generate the 30 dB signal-to-noise needed to successfully lock the first generation CEP phase locking electronics.

There is another method that is being implemented on this next generation scheme. It will allow the ability to synthetically produce a signal-to-noise ratio on the range of 60dB at a 10 kHz

offset. This method uses a narrow band filter to remove the surrounding noise around the CEP beat note. One of the key issues with using a narrow band filter is the selection of the central wavelength. The used beat frequency is one fourth the repetition rate from the oscillator. This then requires the filter to be in the range of 21 MHz. The selection of the exact frequency is then determined by the possibility of manufacturing a filter in this frequency range. In the high frequency (HF) range, the common method for filtering is to use lumped elements (capacitors and inductors). In order to generate a filter with the bandwidth of less than 10 kHz the possibility of using lumped elements is not practical and the use of crystal filters is the preferred method. Crystal filters allows the construction of a filter with a somewhat flat pass band and steep fall offs. This could then allow the ability to generate a 60 dB roll off in the stop band of the filter. Figure 13 is a simulation of the power efficiency of a 6 order crystal latter filter.

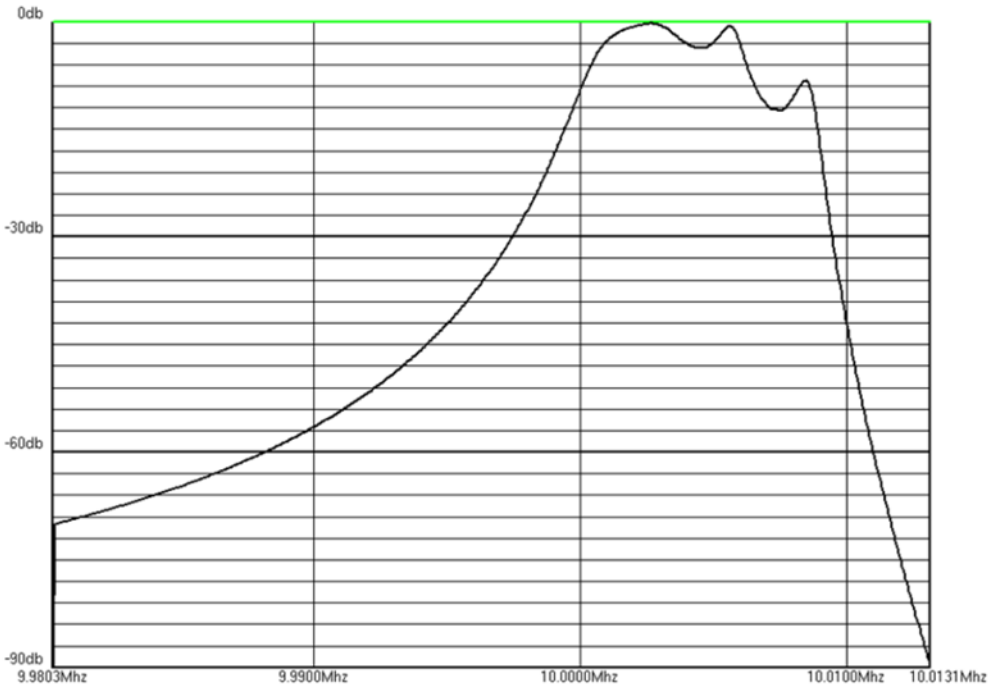

Figure 13: Crystal latter filter with a bandwidth of 10 kHz and improper matching network.

The next step in designing the filter is the selection of the central wavelength. This means that once the filter is designed, the final frequency is set and cannot be adjusted. This is a big problem as the repetition rate of the oscillator changes daily by a few 10 kHz. The main effect that changes the oscillator repetition rate is when tuning to generate the octave-spanning bandwidth needed to perform the f-to-2f measurement. Since the filter bandwidth is extremely narrow compared to the central frequency, having a Q factor of over 2000. This would require multiple filters that span the CEP frequency range. This then states that as the laser drifts by thermal expanding of the laser cavity that the filter used may also need to be changed to accommodate the drifts. For an 85 MHz oscillator with the cavity length of 1.7 meters, the change of 20 microns changes the oscillator frequency by 1 kHz. This change in cavity length is possible in our system since the need to tweak the laser cavity for maximum bandwidth. Therefore if the maximum distance that the laser cavity can change length during a series of tweaking operations could be on the order of a few mm. The adjustments of a few mm of optical cavity would change the frequency of the laser by 120 kHz this would then require 24 filters to cover the ranges with some overlap. Designs of over eight filters make the electronics to control the system too complex. It would require continuous switching of filters to keep the beat frequency locked. A more elegant way to perform this task is to use the same concepts of as a Supper-heterodyne receiver. Here the filter used to remove the out-of-band noise is through the use of an Intermediate Frequency (IF). It allows the ability to filter a wide frequency ranges without the need of switching filters. Figure 14 is the block diagram is the design of this CEP beat frequency cleaning design.

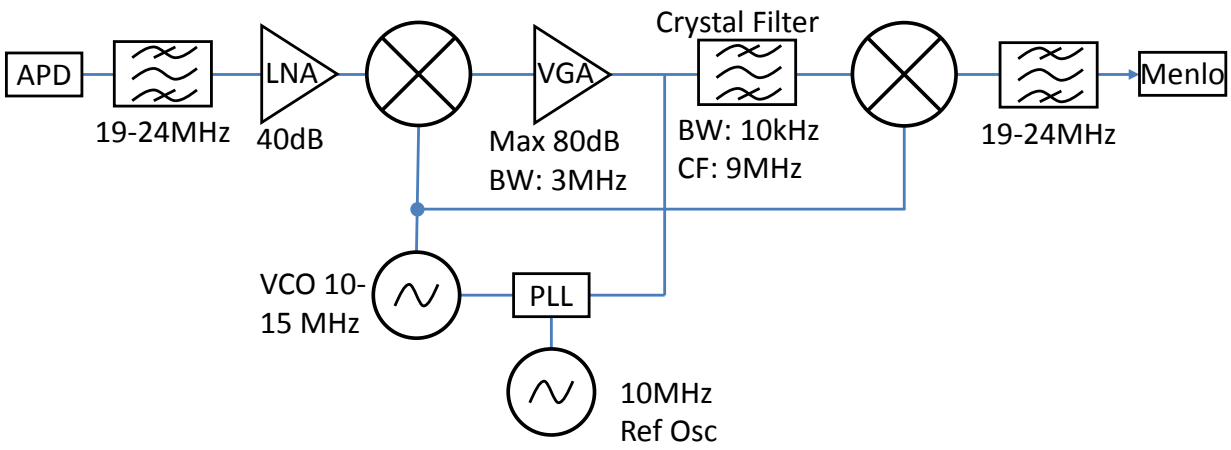

Figure 14: Block diagram of CEP electronics cleaner.

The design of this technique uses a band pass filter with a bandwidth of 6 MHz. The filter removes aliasing frequencies that would then latter interfere with subsequent processes. The next step is to mix the filtered signals with a double balanced ring mixer. This mixer generates the sum and difference in frequencies of the input signals and the local oscillator. The local oscillator is a Variable Frequency Oscillator (VFO) with a frequency range of 11 to 14 MHz. With a CEP beat frequency of 21 MHz the mixing will move the beat frequency to the range of 7 to 10 MHz. The next step is to amplify the signal with about 70 to 90 dB of gain. This variable gain is generated with the help of an Auto Gain Control (AGC) circuit. It would allow a constant output power if the signal drifts by 20 dB and reduces the saturation of the amplifiers. Without the AGC amplification would increase the noise floor without increasing the wanted signal. This signal then is split to the crystal band pass filter and to a set of locking electronics. The locking electronics locks the CEP beat frequency to 9 MHz. The reason to lock the signal to 9 MHz is that this frequency is the IF of the system. The crystal narrow band pass filter is centered to this frequency. This process then would produce a clean output signal with the noise

floor being around 60 dB below the carrier. Figure 15 is the before and after signals of going through the band pass filter and after.

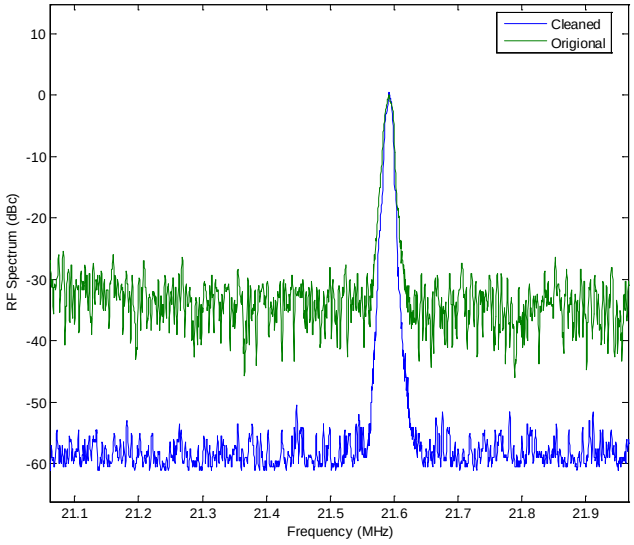

Figure 15: Original and cleaned electrical CEP beat.

At this stage the beat frequency has a clean signal but is centered on 9 MHz, this is not useful for CEP locking. The 9 MHz signal only contains the “fast information” of the CEP beat and the VFO contains the remaining “slow information” of the beat. The next step is to convert the frequency back to the correct CEP beat frequency. The cleaned signal is then mixed again with the same VFO that was used to down convert the tone to the IF frequency. This then generates the correct CEP beat signal with some other products. The final step is to remove the other products from the output. This is done with the same type of filter used in the input of this device. Figure 16 is two RF spectrum waterfalls, were the Y axis is the time and the X axis is the frequency with a window of one megahertz. The time period is 5 minutes. The left waterfall is an unfiltered signal with 30 dB of signal-to-noise ratio. The right waterfall is the clean signal with over 60 dB of signal-to-noise.

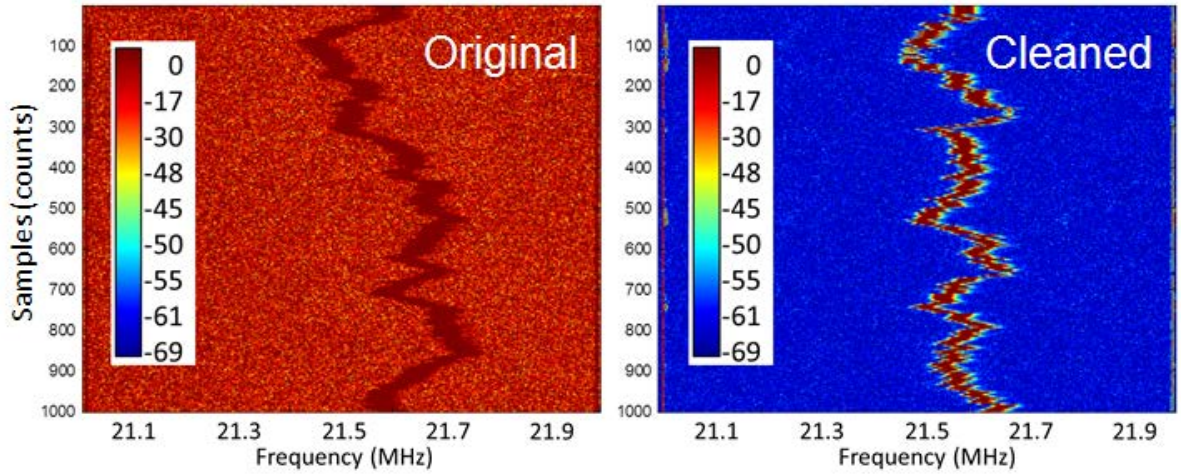

Figure 16: Waterfall of simulated CEP beat in original response and clean with same intensity profile.

The signal used was generated with a computer controlled Direct Digital Synthesizer (DDS). The signal was varied with similar characteristics as an unlocked CEP beat note. This new generation of fast CEP signal conditioner should allow simplified setup compared to the current MenloSystems locking electronics. It also reduced the amount of noise produced by spurs close to the CEP beat note.

3.7 Summary

The control of the CEP output from the oscillator is determined by the used f-to-2f interferometer and the output power from the oscillator. Techniques have been developed to reduce the amount of noise introduced into the measurement of the fast CEP drift tone. They include stabilization of two-arm interferometers and the introduction of collinear interferometers. Additional techniques are currently being implemented to allow lower S/N ratios locking. All of the above techniques improve the CEP locking of the HERACLES laser facility.

4. OUTPUT STABILIZATION OF HERACLES FOR IMPROVED CEP STABILITY

The HERACLES facility is designed to provide a mJ-level pulse energy and sub-10-fs pulse duration [44]. This state-of-the-art OPCPA facility has been improved and upgraded and the current energies are at the µJ-level. The front end of this system is a MenloSystems Inc., Octavius 85M oscillator. It has sub-5-fs pulse duration and 200 mW of average power. The repetition rate from this oscillator is 85 MHz. It allows the system to use the $f_{rep}/4$ signal as a reference in CEP locking measurements. Since the pulse duration is shorter than 5 fs the bandwidth of the oscillator is in the range of >600 nm (full width) and at the wings of the output extends over one octave. The ability to directly perform an f-to-2f interferometer is possible without the need of a spectral broadening. This has the advantage to reduce phase noise that would otherwise originate from the broadening technique. The Oscillators broad bandwidth requires careful alignment during startup. Operating the oscillator in a highly nonlinear regime leads to a reduced crystal lifetime of a few weeks and the position of the crystal needs to be moved perpendicular to the optical axis if damage occurs. Figure 17 is the oscillator of the HERACLES laser facility.

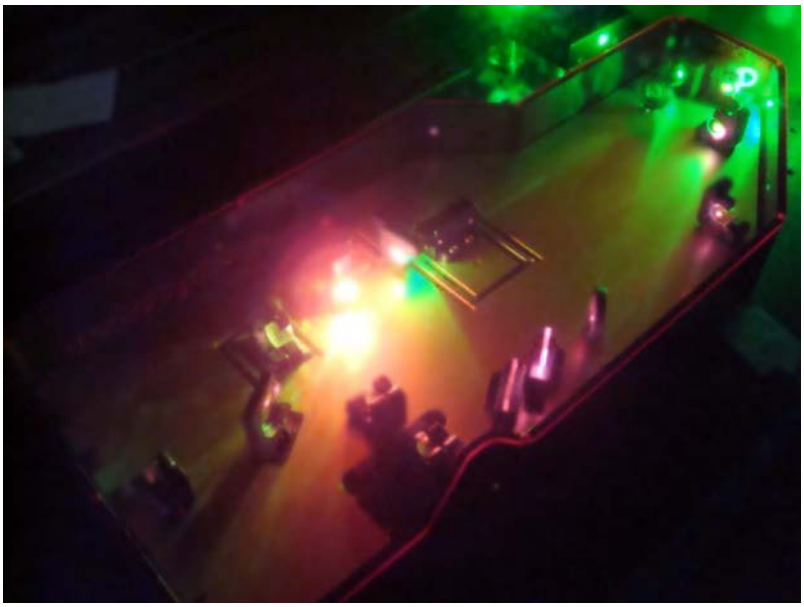

Figure 17: 5-fs laser oscillator for HERACLES.

4.1 First generation of the HERACLES

After the oscillator the output beam is split equally for the generation of a seed and a pump line in the OPCPA design. The OPCPA pump of the system uses an Yb:fiber pre-amplifier to amplify a portion of the spectrum centered at 1064 nm with 3 nm bandwidth. This is not the center gain wavelength in Yb-doped fiber and thus not a highly efficient amplifier setup. This amplification method takes advantage of the off tuning and produces reduced amplified spontaneous emission (ASE) [45].

After the pre-amplifier stage, a pulse picker is used to reduce the repetition rate to 10 kHz and the beam passes into a regenerative amplifier with a gain material Nd:YVO_4. The output energy of the regenerative amplifier is on the order of 0.5 mJ [46]. The output enters a single-pass amplifier, which also used Nd:YVO_4 as gain medium. The design is based on Nd:YVO_4, to

take advantage of the birefringence and the high small signal gain of around 5. The output of this pump line is greater than 2 mJ at 1064 nm. The frequency doubling efficiency is up to 66 %.

It has been found (see Appendix A) that the amplifiers based on these Nd:YVO_4 modules have poor beam pointing stability. A few hundreds μrad of pointing instability in the first amplifier stage continued to compound on top of each additional stage. At the location of the OPA stages the centroid movement of the focused beam was visually noticeable and the focused beam would move by a more than the beam diameter at its waist. As a consequence, a high amount of output power fluctuations in parametric gain was observed. The parametric gain was fluctuating from tens to millions due to the poor overlap. These fluctuations prevented the ability to perform long-term CEP measurements. Measurements showed that the beam pointing fluctuations where introduced by the amplifier module itself. This led to a re-design of the amplifier chain under the special consideration of high beam pointing stability.

4.2 Second Generation of the HERACLES Pump

With the found issues of beam pointing stability and the need for higher output power, a redesign of the regenerative amplifier was necessary. To improve from the previous design the implementation of a feedback system to stabilize the long-term drifting. These upgrades will improve the overall performance of the pump line and could allow the implementation of slow CEP drifts measurements.

4.2.1 Regenerative Amplifier

The need for higher pulse energy from the regenerative amplifier is a requirement since the necessary output energies are needed to perform the slow CEP measurements. Figure 18 is a diagram of the regenerative amplifier used in HERACLES.

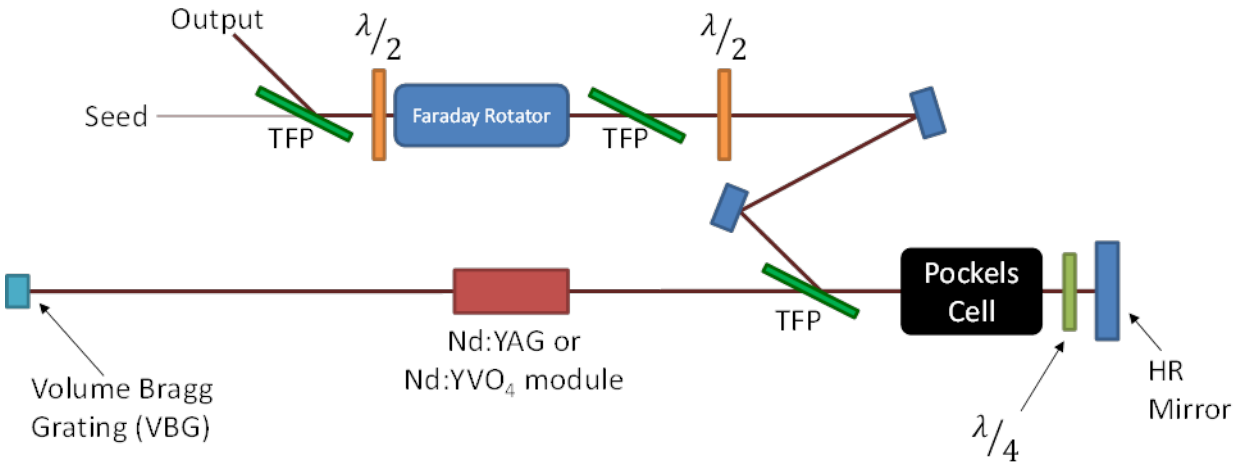

Figure 18: Layout of regenerative amplifier in HERACLES.

$Nd:YVO_4$ with a SSG of 5 outperforms Nd:YAG with a SSG of 2.3 in the amplification of small signals. In contrast, with low repetition rates (below 4 kHz) the Nd:YAG module outputs higher energies than $Nd:YVO_4$ in a regenerative amplifier. The final results of a regenerative amplifier cavity for each module are shown in the Figure 19.

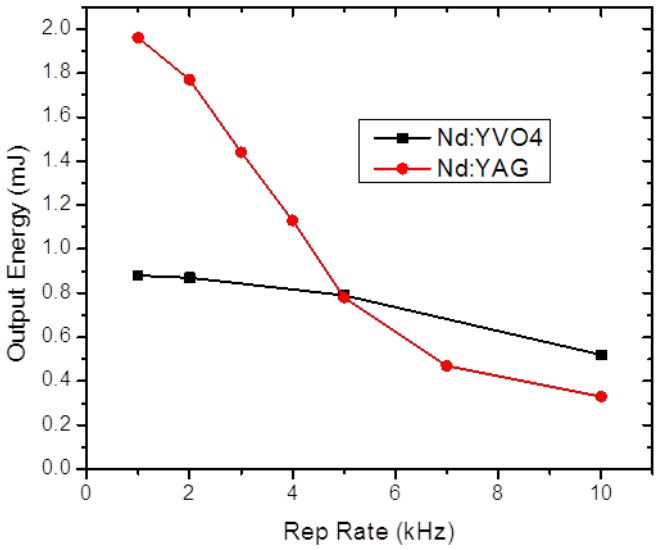

Figure 19: Output energies of a Nd:YVO_4- and Nd:YAG-based regenerative amplifier.

A drawback when using Nd:YAG is the upper state lifetime of 230 μs [47]. This limits the repetition rate of the regenerative amplifier. As the repetition rate of the system extends beyond the 4.3 kHz mark the output power approaches the CW output power of the Nd:YAG regenerative amplifier. Since the limitation of available sizes of Nd:YVO_4, the future amplifiers that will be used for this system will be Nd:YAG. To build the system for having higher output energy and allows for future upgrades the system is ran at 3 kHz. Running the system at 3 kHz, Figure 17 shows that the maximum output energy is with Nd:YAG module.

The next task for optimizing the regenerative amplifier is the long-term and short-term stability of the output power. The reason for the short-term stability of the system is that for the first OPA the pump and seed used is tightly focused to allow the highest gain with minimal fluorescence. The intensities in the BBO crystal are approaching the ionization threshold of the material. If the pump beam was not stable, an increase in energy would be beyond the ionization

threshold of the BBO. This would damage the crystal and require realignment. To generate a stable pulse-to-pulse stability from the regenerative amplifier the second saturated pulse from the cavity buildup is selected. Figure 20 is the cavity build-up of the seed as it is amplified through the regenerative amplifier without dumping the cavity.

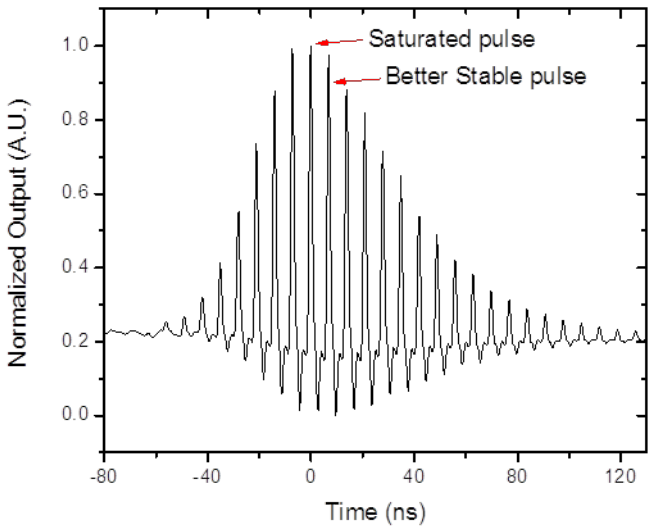

Figure 20: Temporal gain profile of a regenerative amplifier. For the measurement a leaked signal is picked up with a fast photo diode.

When selecting the output pulse from the regenerative amplifier cavity, there is always a tradeoff in selecting the pulse with the highest energy and stability. As the time increases for the trapped seed to travel through the regenerative amplifier, it will continue building up energy. At some point the losses in the amplifier begin to overpower the gain. After the pulse extracts the maximum output energy the following pass that the pulse travels begins to loose energy. The energy of the pulse becomes increasingly more consistent to previous pulses as it remains trapped in the regenerative amplifier with the drawback of lower energy. The round trip that

produces the best trade-off of both high output energies and a stable pulse-to-pulse energy is the second pulse after it has reached its saturation.

As stated in the previous section the long-term stability of the output from the regenerative amplifier can drift lightly. The change can occur through thermal drifts in the cavity, instabilities in the seed. One method to compensate for these drifts is to build the regenerative amplifier on a temperature controlled breadboard and reduce the amount of other noises that could be introduce into the laser cavity, such as turbulent air flow. The simplest method that was implemented was the use of metal boxes to reduce the air turbulences and reduce the RF noise produced by the Pockels Cell used to inject and dump the seed. Another implementation that was introduced into the regenerative amplifier is a feedback system that monitored the output energy. It compensated the output by controlling the pump power of the Nd:YAG module. First it was determined if controlling of the pump current could be used to stabilize the output of the regenerative amplifier. Figure 21 is the short term laser output of the regenerative amplifier with a change in pump current.

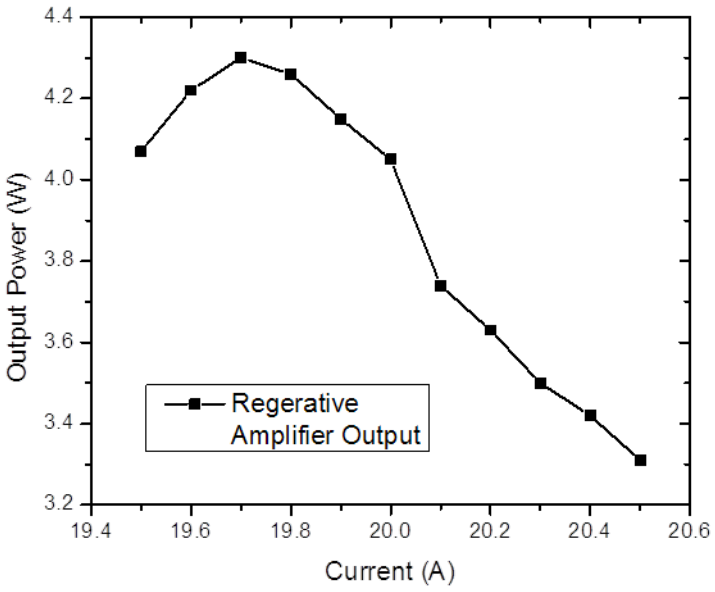

Figure 21: Dependence of pump current on the output power of the regenerative amplifier.

With changing the pump current it is possible to change the output of the regenerative amplifier without the need of a dramatic change in current. This then would allow the ability to create active feedback to compensate for thermal drifts and other noises that would otherwise create fluctuations in the output. The negative slope is due to a constant time selection of the output pulse. With increase in gain the saturation pulse occurs sooner and the pulse that is removed has lost more energy. A simple feedback system was implemented to test if the controlling the pump current could be used for stabilization. Figure 22 is the output before compensation. The data was collected with a fast photodiode and a 10 bit ADC. The step resolution was limited and may have generated larger fluctuations then actually produced.

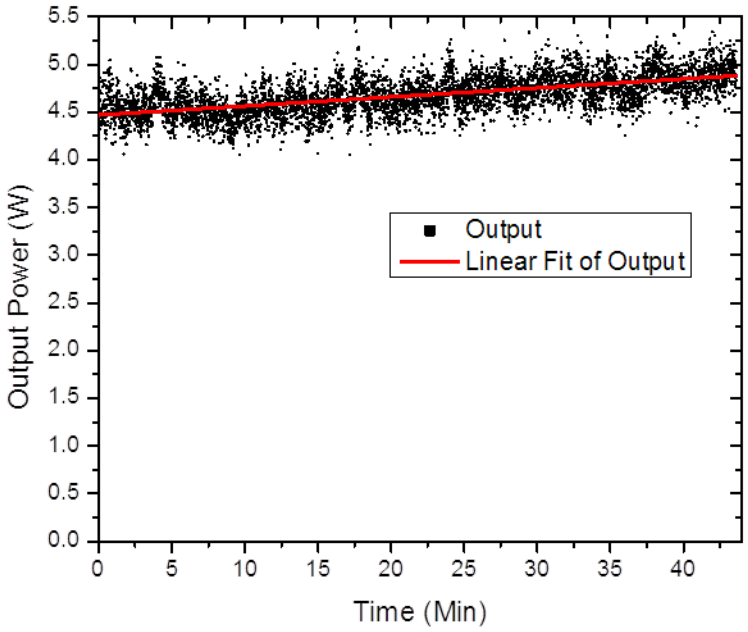

Figure 22: Output energy from pump line with no feedback to compensate for long-term drifts.

The feedback system that was implemented was a simple circuit that measured the output of the regenerative amplifier using a thermal power meter. It then sent 15 data points per second back to the computer. It reduces the shot-to-shot fluctuations and gives less control of the fast changes that the regenerative amplifier may produce but allows long-term improvements. Computer software was written to control the output current of the driving power supply of the Nd:YAG module. The initial version of the code consisted of a simple check that determined if the output power drifted up or down. It then sends to the laser power supply a corresponding current that would compensate for the change. Figure 23 is the stabilization of the output using the above procedure.

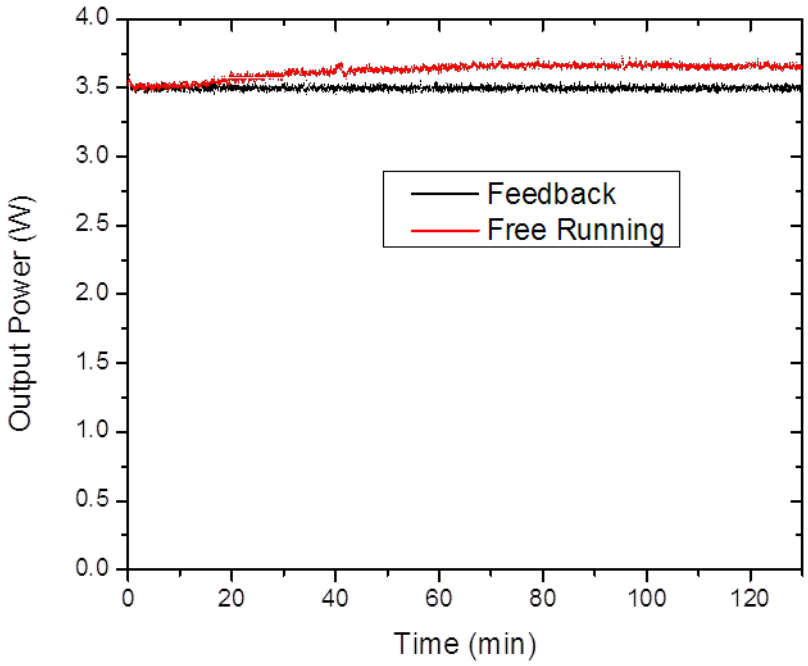

Figure 23: Stabilized output from pump line.

This shows that with the simple feedback system it is possible to stabilize the output energy of the regenerative amplifier. Free-funning drifting of the output energy was on the order of 1.4 % and with the feedback system the output energy has reduce to an overall fluctuation of 0.4 %. This three times increase in stability could be improved with a better feedback loop that incorporates a full PID loop and a faster detector with higher resolution. The new design for monitoring and controlling the feedback of the regenerative amplifier will consist of a fast photodiode with an acquisition unit with a bit size of 24 allowing the measurement accuracy of 0.18 µV.

4.2.2 Single-Pass Amplifier

An improved Nd:YVO_4 module is used to generate the higher output energy from the pump line. The pointing stability was proven to be the highest of all the modules and the small signal gain through the module is ~ 5. Both of these advantages are taken and the module is used as a single pass amplifier after the regenerative amplifier. Another advantage of using Nd:YVO_4 as an amplifier is the polarization maintaining properties. It allows the ability to generate high gain without depolarization is usually induced in Nd:YAG amplifiers. Figure 24 is the output energy produced with different pumping currents of the single pass module. The seed energy was 0.93 mJ. The maximum output energy with the Nd:YVO_4 module is around 2.9 mJ at 1064 nm center wavelength.

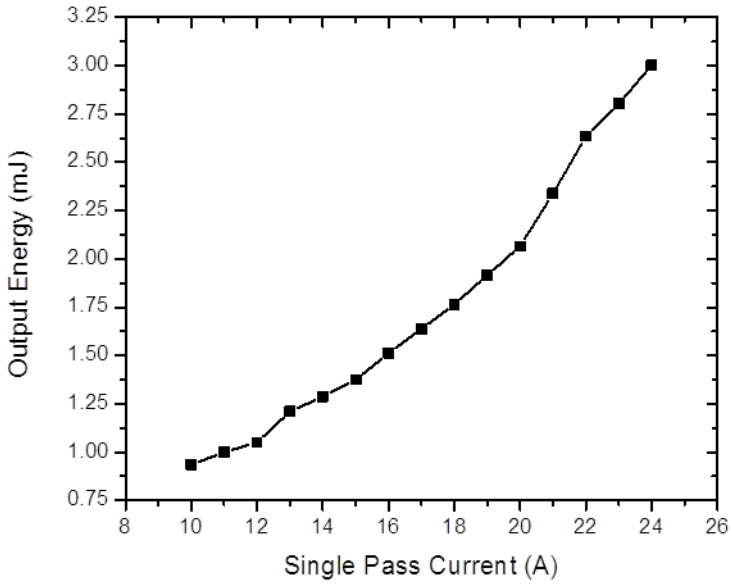

Figure 24: Output Energy from single pass amplifier in dependence of the pump current.

Since the subsequent stage in the pump line requires the output to be collimated, the thermal lensing must be kept constant. Since a feedback is now used to correct for fluctuations of

the output of the regenerative amplifier, this stabilized the divergence of the single-pass. A corrector lens was placed one focal distance away from the focus and allows a collimation of the output beam. With the design of this corrector system a telescope was constructed. The selection of collimating lens is used to expand or reduce the output beam size. The single-pass amplifier is followed by a Second Harmonic Generation (SHG) stage. It is used to up-convert the IR light from the single pass to 532 nm. The optimization in size of the beam was determined through the conversion efficiency of the SHG. With proper alignment and optimization of collimation a conversion efficiency of 66 % was. During repeated power cycles and without tweaking the system, a conversion efficiency of at least 60 % with a drift of three percent was maintained without any feedback systems. Once the feedback system is finalized the drift in conversion efficiency will be reduced.

4.2.3 Long Term Stabilization of Seed for the Regenerative Amplifier

The output energy of the pump in HERACLES needs to be stable to allow a constant gain in the OPA stages. The key to generate a stable pump is to first start with a stable seed. The pre-amplifier used in this system has two options that could allow modification of the output power of the seed. The first is temperature tuning of the pump diode. Since the response time is long and the dynamic range is low, this is not implemented. The second method is the control of the pump current of the diode. This method allows the maximum control of the output of the seed. Figure 25 is the direct measurement of the seed energy compared to the drive current of the diode.

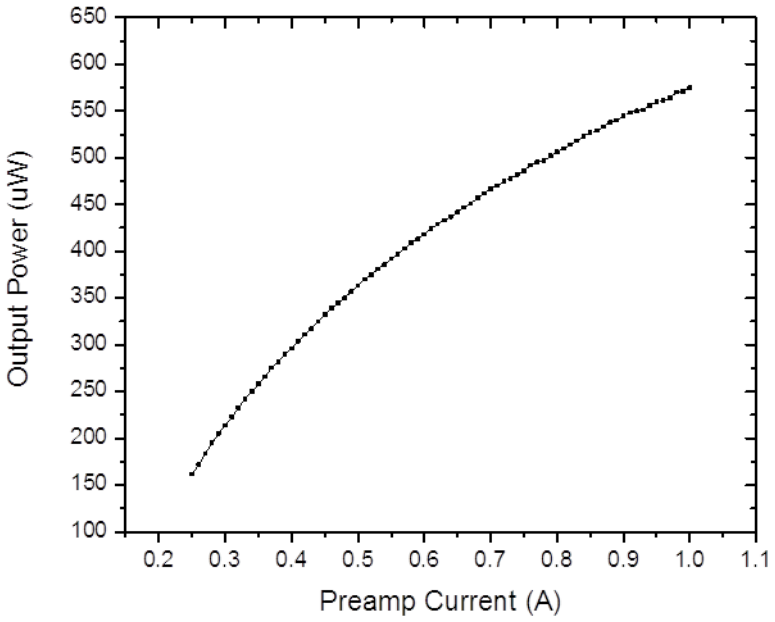

Figure 25: Direct measurement of pre-amplifier output with changing the driving diode current.

It is important to notice that as the fiber amplifier reach the onset of pump saturation around 0.7 A, indicated by the reduced slope in gain at this range. At around 0.2 to 0.3 A, the slope is steeper and will allow a higher control of the power fluctuation of the seed. Also, operating initially at lower amplification gives a ~50 % margin for the case the seed drops significantly in power.

The first design of stabilizing the output of the regenerative amplifier was to control the seed input and monitor the output of the regenerative amplifier. This method then requires that if there are any drifts in the regenerative amplifier then the seed input must be able to compensate for this. Figure 26 is the measurement of the output of the regenerative amplifier, while tuning the seed. The reason for the increase in output energy with reducing the seed energy is a consequence of moving the buildup time in the cavity. Since the selected pulse that is kicked out

of the regenerative amplifier is the more stable second pulse, as the energy decreases this pulse begins to become the first saturated pulse. This pulse is less stable in shot-to-shot, but has more output energy. Any seed energy below 1pJ the regenerative amplifier behaves as a q switch oscillator and the resulting output is unusable for this OPCPA system.

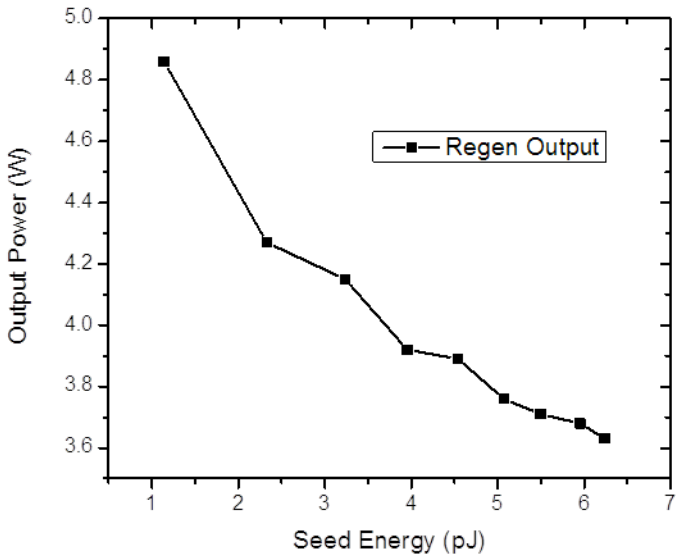

Figure 26: Regenerative amplifier output in dependence of pre-amplifier seed.

To stabilize the system, the default current of the pump diodes started at 0.2 A, this was in the range with the highest slope. Then a portion of the output from the regenerative amplifier was collected by a photodiode. The signal from the photodiode then was sent through a peak detector that allowed an analog to digital converter (ADC) to sample the signal without the need of precise timing. The output of the ADC was then passed to the computer using the USB port. The use of the USB allows the ability to measure each of the output pulses from the regenerative amplifier at 3 kHz with a 10 bit resolution. With a LabView program a PID loop was created to adjust the pump current of the pre-amplifier. A new design is currently being introduced into the

seed feedback system that adjusts the seed power. This would then allow the precise measurement and control of the seed without adding the variables of the regenerative amplifier. Figure 27 is the response of the output power of the seed compared to the response of the APD.

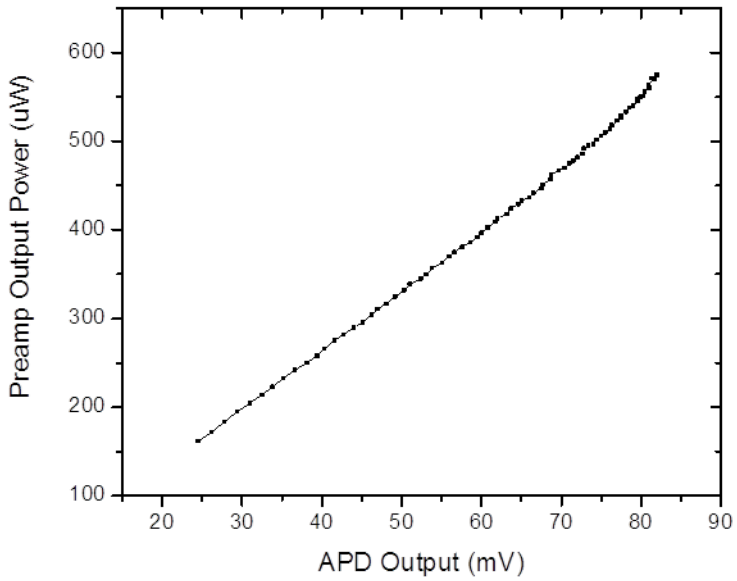

Figure 27: APD response of pre-amplifier output powers.

4.3 Future Improvements to Increase the OPCPA Pump Power

The initial design goal for the output power of the HERCLES laser facility was estimated to be 0.2 TW. The booster amplifier that was originally designed for the project included 1 cm Nd:YAG modules. The limitation in using this design was given by the small signal gain is of 1.3. Another limitation was the strong depolarization that occurred with these modules. With the two issues the initial design goal was not reachable. It led to the development of utilizing smaller Nd:YAG modules of 3 mm diameter with a small signal gain of 2.5. With the increased gain and with a depolarization compensation scheme, a new amplifier was designed. Once this design is

implemented the pump line should increase to 33 mJ giving a total gain of 17 for the booster amplifier system. For the analysis of pulse-to-pulse stability of the amplifier system, it was determined that the last passes through the final amplifier will be approaching saturation. Figure 26 is a simulated output response for a given input energy taking into account the saturation of the system.

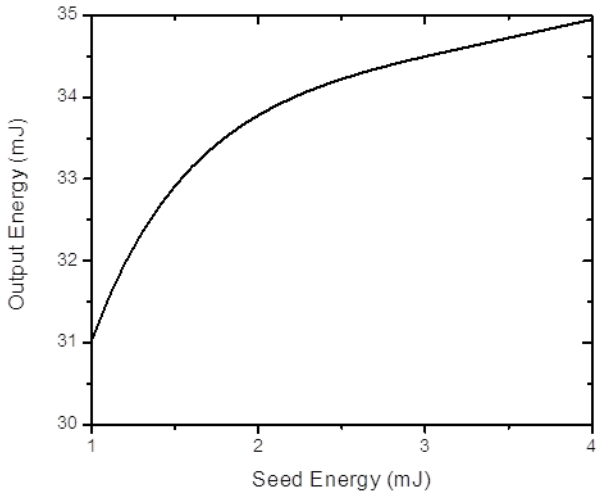

Figure 28: Simulated output characteristics of the next booster upgrade.

It shows that for a pulse fluctuation of 5 % the output pulse fluctuation would be less than 0.3 %. It would greatly increase the final output energy of HERACLES and improve the pulse-to-pulse stability allowing stable slow CEP measurement.

4.4 Redesign of the OPAs for Higher Pump Energies

The old design needed to generate gain in the OPA required tight focusing could not be used since the increase of the output powers of the regenerative amplifier and the single-pass amplifiers. With the increase in pump power the tight focusing of the old setup would damage

the BBO crystal. It gives to two options for the redesign of the OPA. The first option relies on recycling the pump beam and using it to pump a second OPA for additional gain. The necessary change would be a change of the focal length in the pump beam, so that it would not damage the BBO but achieve sufficient intensity. With preliminary results the final gain of the system was on the order of 3×10^6. The fluorescence that was generated was extremely high on the orders of the seed output. This shows that the matching of the pump and seed beam diameters was low during the initial OPA setup. It leads to the fundamental limitation of this design, that to allow for maximum gain of the system more energy needs to pass through the first OPA generating a high amount of SF and only generating minimal seed gain through the second OPA.

A better option that will reduce the amount of SF on the first OPA is to split the pump beam. Here the pump beam is passed through a light valve that consists of a thin-film polarizer (TFP) and a half-wave plate (HWP). The valve redirects a portion of the beam to the first OPA and the remainder to the second OPA. This design allows tighter focusing at the first OPA reducing the SF and giving the second OPA a clean seed. This method is currently being implemented.

4.5 Summary

Improvements in energy stability from the output of the pre-amplifier, the increase in output power of the regenerative amplifier stage and increased pointing stability of the pump beam have enhanced the HERACLES system performance. Increasing the energy and stability of the pump beam allows increasing the stability of the final OPCPA beam. A stable OPCPA beam allows the measurement of the slow CEP drift that was previously not measurable. Future implementation of the booster amplifiers will push the HERACLES facility closer to its design

goal of 0.2 TW. Analysis shows that as the amplifier system approaches saturation the shot-by-shot stability of the system improves.

5 CONCLUSION

Ultra-fast, high-intensity laser fields have many applications ranging from HHG and attoscience to particle acceleration. Building a table-top laser system to enable these applications led to the current advances in CPA and OPCPA laser systems. Both techniques nowadays support pulse durations approaching the quasi-single-cycle regime. Many of the applications require precise control of the CEP since a phase shift of few hundred microili-radians results in a change in maximum electric field strength. Thus, stabilization of the CEP to minimal drifts during experiments and generation of a high-quality, few-cycle, high-energy laser output is desired for these applications.

This thesis shows the avenues taken to move HERACLES to a high-energy, few-cycle laser facility with precise CEP control. The first part of this thesis shows the improvements and results ultimately leading to ultra-reliable, long-duration CEP stabilization. Over 30 dB of signal-to-noise was required for locking in the first generation of the CEP stabilization scheme used for HERACLES. The introduction of innovative improvements in the measurement electronics similar to super heterodyning reduced the out-of-band noise to more than 60 dB. This synthetically increased signal-to-noise ratio and signal quality allows locking of the CEP frequency far below the original 30 dB requirement. It leads directly to CEP locking with ultra-high reliability especially benefiting long-duration experiments.

The second part of this thesis describes the implemented improvements and results towards high-quality OPCPA pump beam generation. This effort directly enables the generation

of high-quality and highly stable output performance of the high-energy, few-cycle laser facility HERACLES. In this thesis, the causes are identified limiting the OPCPA output quality with the first pump beam generation. These included issues to stabilize the CEP and poor beam pointing stability of the pump beam generation. Investigations of the origins and the implemented solutions are addressed in this thesis. In the second generation, the re-design of the regenerative amplifier improved the overall stability of the system as well as increased the energy to above 1 mJ. The implemented single-pass, power amplifier has improvements in beam pointing and final output energy of 1.8 mJ at 532 nm was obtained. Implementation of feedback-control reduced the long-term power drift of the pump line to less than 0.5 %. These modifications improved the OPCPA pulse-to-pulse and long-term stability.

The work presented in this thesis on CEP stabilization and improved pump beam generation directly improve the performance of the HERACLES facility. The OPCPA system is designed to provide several mJ pulse energy and a few kHz and sub-10-fs pulse duration. The pulse-to-pulse stability of this facility is improved by major re-designs of CEP electronics as well as pump beam generation. The long duration stability is also largely improved by these implementations. Additional feedback loops provide excellent control of the overall performance of the OPCPA output. In conclusion, the presented improvements of the HERACLES facility enable the next generation of experiments with quasi-single cycle pulses and high pulse energy.

APPENDIX A:
BEAM POINTING INVESTIGATIONS

A major issue with the first design of the HERACLES system was the walking of the pump beam. It prevented the ability to measure slow CEP and hindered the output performances of the laser system. An investigation of the of the pump beam pointing, led to the discovery that the regenerative amplifier's original Nd:YVO_4 module was the largest contributor. To solve this issue an investigation of the beam pointing was performed on each module. Figure 29 shows how each module preformed with respect to the pumping intensity.

The data clearly shows that to create a stable laser system the module with lowest beam pointing would be the newer Nd:YVO_4 module and the second best module would be the Nd:YAG module running at the highest flow rate possible. There are other possible design changes that will be implemented in the following sections that greatly improve the laser system and will allow the ability to implement slow CEP locking.

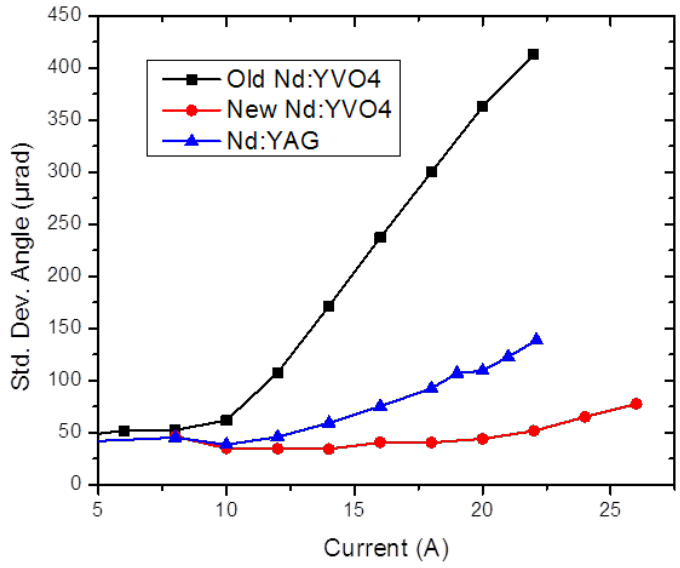

Figure 29: Pointing Stability of the used laser modules.

Another performance test was performed to determine how flow rate changed the pointing stability of the module. It was concluded that as the flow rate increased the walking of the beam decreased as shown in Figure 30. This seemed to be counterintuitive since the increase in flow rate usually introduces more noise.

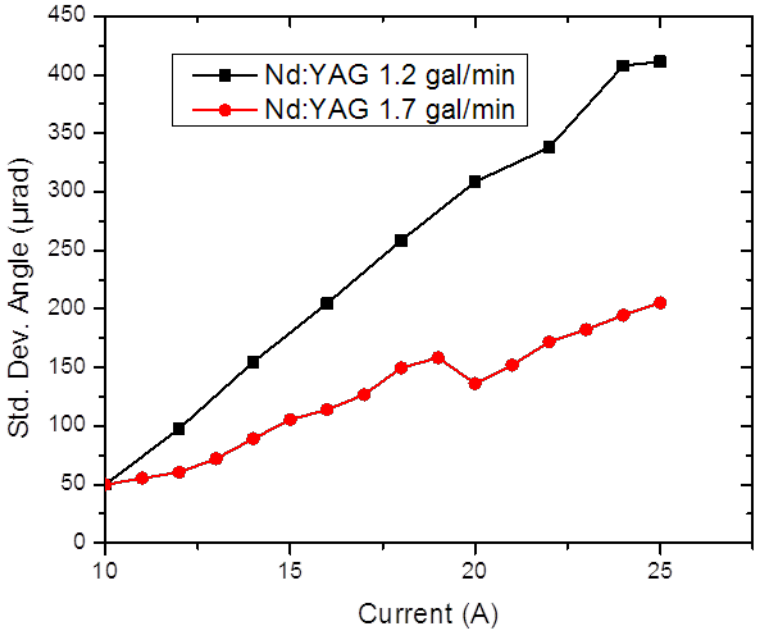

Figure 30: Pointing stability with different flow rates.

APPENDIX B:
LIST OF PUBLICATIONS AND CONFERENCE CONTRIBUTIONS

Benjamin Webb, Andreas Vaupel, Michaël Hemmer, Nathan Bodnar, and Martin Richardson, "Next generation high power OPCPA femtosecond laser systems," DEPS Ultrashort Laser Workshop In Santa Fe, NM, USA (June 2011)

Benjamin Webb, Andreas Vaupel, Nathan Bodnar, Lawrence Shah, and Martin Richardson, "Scaling CPA and OPCPA lasers to beyond 10 TW level," CREOL Industrial Affiliate day 2011, Orlando, FL, USA (April 2011)

Andreas Vaupel, Benjamin Webb, Nathan Bodnar, Lawrence Shah, and Martin Richardson, "Two Paths for OPCPA Laser Development: High Average Power vs. High Pulse Energy," CREOL Industrial Affiliate day 2011, Orlando, FL, USA (April 2011)

Andreas Vaupel, Nathan Bodnar, Benjamin Webb, Michaël Hemmer, and Martin Richardson, "Design and preliminary results for a sub-5-fs, 100 mJ-level, CEP-stabilized laser facility - PhaSTHEUS," High Intensity Lasers and High Field Phenomena (HILAS), Istanbul, Turkey (February 2011)

Andreas Vaupel, Nathan Bodnar, Michaël Hemmer, and Martin Richardson, "A Joule-class, TEM00 spatial Profile, Narrow-Linewidth Laser System," Proceedings of the SPIE, Solid State Lasers XX: Technology and Devices, SPIE Photonics West – LASE, San Francisco, CA, USA (January 2011)

Nathan Bodnar, Julien Nillon, Eric Cormier and Martin Richardson "A Dual-pumping Geometry for Non-collinear Optical Parametric Amplification," SYMPOSIUM ON UNDERGRADUATE RESEARCH, Division of Laser Science of A.P.S - LS XXVI - Rochester, NY 25 (October 2010)

Danielle Simmons, Nathan Bodnar, Matthieu Baudelet, and Martin Richardson, "Fourier Transform Infrared Spectroscopy," SYMPOSIUM ON UNDERGRADUATE RESEARCH, Division of Laser Science of A.P.S - LS XXVI - Rochester, NY, 25 (October 2010)

Reuvani Kamtaprasad, Omar Rodriguez, Nathan Bodnar, John Szilagyi, Moza Al-Rabban and Martin Richardson, "EUV Spectral Analysis of Laser Plasmas from Sn, In, and Sb-doped Droplet Sources," CREOL Industrial Affiliate day 2010, Orlando, FL, USA (April 2010)

Nathan Bodnar, John Szilagyi, Omar Rodriguez, Reuvani Kamtaprasad, and Martin Richardson, "Generation of Stable Droplets for EUV Plasma," SYMPOSIUM ON UNDERGRADUATE RESEARCH, Division of Laser Science of A.P.S - LS XXV – San Jose, CA (October 2009)

LIST OF REFERENCES

[1] L. Xu, C. Spielmann, A. Poppe, T. Brabec, F. Krausz, and T. W. Hansch, "Route to phase control of ultrashort light pulses," Optics Letters **21**, 2008-2010 (1996).

[2] Z. Chang, "Single attosecond pulse and xuv supercontinuum in the high-order harmonic plateau," Physical Review A **70**, 043802 (2004).

[3] M. Kresz, T. Loffler, M. D. Thomson, R. Dorner, H. Gimpel, K. Zrost, T. Ergler, R. Moshammer, U. Morgner, J. Ullrich, and H. G. Roskos, "Determination of the carrier-envelope phase of few-cycle laser pulses with terahertz-emission spectroscopy," Nature Physics **2**, 327-331 (2006).

[4] A. Suda, M. Hatayama, K. Nagasaka, and K. Midorikawa, "Generation of sub-10-fs, 5-mJ-optical pulses using a hollow fiber with a pressure gradient," Applied Physics Letters **86**, 111116 (2005).

[5] M. Schultze, T. Binhammer, G. Palmer, M. Emons, T. Lang, and U. Morgner, "Multi-µJ, CEP-stabilized, two-cycle pulses from an OPCPA system with up to 500 kHz repetition rate," Optics Express **18**, 27291-27297 (2010).

[6] A. Vaupel, N. Bodnar, B. Webb, M. Hemmer, and M. Richardson, "Design and preliminary results for a sub-5-fs, 100 mJ-level, CEP-stabilized laser facility - PhaSTHEUS," in OSA Technical Digest (CD) (Optical Society of America, 2011), HThE5.

[7] S. Adachi, N. Ishii, T. Kanai, A. Kosuge, J. Itatani, Y. Kobayashi, D. Yoshitomi, K. Torizuka, and S. Watanabe, "5-fs, multi-mJ, CEP-locked parametric chirped-pulse amplifier pumped by a 450-nm source at 1 kHz," Optics Express **16**, 14341-14352 (2008).

[8] A. J. Verhoef, J. Seres, K. Schmid, Y. Nomura, G. Tempea, L. Veisz, and F. Krausz, "Compression of the pulses of a Ti:sapphire laser system to 5 femtoseconds at 0.2 terawatt level," Applied Physics B **82**, 513-517 (2006).

[9] E. Žeromskis, A. Dubietis, G. Tamošauskas, and A. Piskarskas, "Gain bandwidth broadening of the continuum-seeded optical parametric amplifier by use of two pump beams," Optics Communications **203**, 435-440 (2002).

[10] P. Fourier, "Théorie analytique de la chaleur," (1822).

[11] R. Holzwarth, T. Udem, T. W. Hansch, J. C. Knight, W. J. Wadsworth, and P. S. J. Russell, "Optical frequency synthesizer for precision spectroscopy," Physical Review Letters **85**, 2264-2267 (2000).

[12] S. A. Diddams, L. Hollberg, L.-S. Ma, and L. Robertsson, "Femtosecond-laser-based optical clockwork with instability <6.3 E 10–16 in 1 s," Optics Letters **27**, 58-60 (2002).

[13] TrabesingerAndreas, "Nobel Prize 2005: Glauber, Hall and Hansch," Nature Physics **1**(2005).

[14] H. R. Telle, G. Steinmeyer, A. E. Dunlop, J. Stenger, D. H. Sutter, and U. Keller, "Carrier-envelope offset phase control: A novel concept for absolute optical frequency measurement and ultrashort pulse generation," Applied Physics B-Lasers and Optics **69**, 327-332 (1999).

[15] P. Lan, E. J. Takahashi, and K. Midorikawa, "Isolated-attosecond-pulse generation with infrared double optical gating," Physical Review A **83**, 063839 (2011).

[16] K. Zhao, Q. Zhang, M. Chini, Y. Wu, X. Wang, and Z. Chang, "Tailoring a 67 attosecond pulse through advantageous phase-mismatch," Optics Letters **37**, 3891-3893 (2012).

[17] C. Altucci, R. Esposito, V. Tosa, and R. Velotta, "Single isolated attosecond pulse from multicycle lasers," Optics Letters **33**, 2943-2945 (2008).

[18] C. Liu, Y. Zheng, Z. Zeng, P. Liu, R. Li, and Z. Xu, "Chirped polarization-gating technique for isolated attosecond pulse generation," Laser Physics **19**, 1600-1606 (2009).

[19] F. Calegari, F. Ferrari, M. Lucchini, C. Vozzi, S. Stagira, G. Sansone, and M. Nisoli, "Efficient attosecond pulse generation by gating HHG with sub-cycle ionization dynamics," in OSA Technical Digest (CD) (Optical Society of America, 2011), CG5_2.

[20] E. Gagnon, I. Thomann, A. Paul, A. L. Lytle, S. Backus, M. M. Murnane, H. C. Kapteyn, and A. S. Sandhu, "Long-term carrier-envelope phase stability from a grating-based, chirped pulse amplifier," Optics Letters **31**, 1866-1868 (2006).

[21] L. Canova, X. W. Chen, A. Trisorio, A. Jullien, A. Assion, G. Tempea, N. Forget, T. Oksenhendler, and R. Lopez-Martens, "Carrier-envelope phase stabilization and control using a transmission grating compressor and an AOPDF," Optics Letters **34**, 1333-1335 (2009).

[22] D. Strickland and G. Mourou, "Compression of amplified chirped optical pulses," Optics Communications **55**, 447-449 (1985).

[23] A. Dubietis, G. Jonušauskas, and A. Piskarskas, "Powerful femtosecond pulse generation by chirped and stretched pulse parametric amplification in BBO crystal," Optics Communications **88**, 437-440 (1992).

[24] I. N. Ross, P. Matousek, G. H. C. New, and K. Osvay, "Analysis and optimization of optical parametric chirped pulse amplification," Journal of the Optical Society of America B-Optical Physics **19**, 2945-2956 (2002).

[25] B. Zhao, X. Liang, Y. Leng, C. Wang, Y. Jiang, J. Du, and Z. Xu, "Optimization of optical parametric chirped pulse amplification with different pump wavelengths," Optics Communications **259**, 137-141 (2006).

[26] J. Zhou, C. P. Huang, M. M. Murnane, and H. C. Kapteyn, "Amplification of 26-fs, 2-TW pulses near the gain-narrowing limit in Ti:sapphire," Optics Letters **20**, 64-66 (1995).

[27] P. Kumbhakar and T. Kobayashi, "Ultrabroad-band phase matching in two recently grown nonlinear optical crystals for the generation of tunable ultrafast laser radiation by type-I noncollinear optical parametric amplification," Journal of Applied Physics **94**, 1329 (2003).

[28] S. Witte, R. T. Zinkstok, W. Hogervorst, and K. S. E. Eikema, "Numerical simulations for performance optimization of a few-cycle terawatt NOPCPA system," Applied Physics B **87**, 677-684 (2007).

[29] N. Boeuf, D. Branning, I. Chaperot, E. Dauler, S. Gue´rin, G. Jaeger, A. Muller, and A. Migdall, "Calculating characteristics of noncollinear phase matching in uniaxial and biaxial crystals," Optical Engineering **39**, 1016-1024 (2000).

[30] X.-L. Li, H.-J. Liu, H.-Y. Wang, W. Zhao, and S.-X. Shi, "Control of the superfluorescence for compact optical parametric chirped pulse amplification," Journal of Modern Optics **55**, 1795-1800 (2008).

[31] F. Tavella, A. Marcinkevičius, and F. Krausz, "Investigation of the superfluorescence and signal amplification in an ultrabroadband multiterawatt optical parametric chirped pulse amplifier system," New Journal of Physics **8**, 219-219 (2006).

[32] F. W. Helbing, G. Steinmeyer, J. Stenger, H. R. Telle, and U. Keller, "Carrier-envelope-offset dynamics and stabilization of femtosecond pulses," Applied Physics B: Lasers and Optics **74**, s35-s42 (2002).

[33] A. Apolonski, A. Poppe, G. Tempea, C. Spielmann, T. Udem, R. Holzwarth, T. W. Hansch, and F. Krausz, "Controlling the phase evolution of few-cycle light pulses," Physical Review Letters **85**, 740-743 (2000).

[34] J. K. Ranka, R. S. Windeler, and A. J. Stentz, "Visible continuum generation in air-silica microstructure optical fibers with anomalous dispersion at 800 nm," Optics Letters **25**, 25-27 (2000).

[35] E. E. Serebryannikov, A. M. Zheltikov, N. Ishii, C. Y. Teisset, S. Köhler, T. Fuji, T. Metzger, F. Krausz, and A. Baltuška, "Soliton self-frequency shift of 6-fs pulses in photonic-crystal fibers," Applied Physics B **81**, 585-588 (2005).

[36] R. A. Fisher and W. K. Bischel, "Numerical studies of the interplay between self-phase modulation and dispersion for intense plane-wave laser pulses," Journal of Applied Physics **46**, 4921-4934 (1975).

[37] V. V. Krishnamachari, E. R. Andresen, S. R. Keiding, and E. O. Potma, "An active interferometer-stabilization scheme with linear phase control," Optics Express **14**, 5210-5215 (2006).

[38] E. Moon, C. Li, Z. Duan, J. Tackett, K. L. Corwin, B. R. Washburn, and Z. Chang, "Reduction of fast carrier-envelope phase jitter in femtosecond laser amplifiers," Optics Express **14**, 9758-9763 (2006).

[39] K. Yamane, T. Naoi, A. Suguro, R. Morita, M. Yamashita, K. Sugiyama, and M. Kitano, "Generation of carrier-envelop-phase stabilized 3.3-fs optical pulses," in *Lasers and Electro-Optics Europe, 2005. CLEO/Europe. 2005 Conference on*, 2005), 384.

[40] C. Yun, S. Chen, H. Wang, M. Chini, and Z. Chang, "Temperature feedback control for long-term carrier-envelope phase locking," Applied Optics **48**, 5127-5130 (2009).

[41] E. B. Kim, J. H. Lee, L. T. Trung, W. K. Lee, D. H. Yu, H. Y. Ryu, C. H. Nam, and C. Y. Park, "Demonstration of an optical frequency synthesizer with zero carrier-envelope-offset frequency stabilized by the direct locking method," Optics Express **17**, 20920-20926 (2009).

[42] S. Rausch, T. Binhammer, A. Harth, and U. Morgner, "Octave-Spanning Ti:sapphire Laser Locked to Carrier-Envelope-Offset Frequency Zero," in OSA Technical Digest (CD) (Optical Society of America, 2010), CWJ2.

[43] T. J. Yu, K. H. Hong, H. G. Choi, J. H. Sung, I. W. Choi, D. K. Ko, J. Lee, J. Kim, D. E. Kim, and C. H. Nam, "Precise and long-term stabilization of the carrier-envelope phase of femtosecond laser pulses using an enhanced direct locking technique," Optics Express **15**, 8203-8211 (2007).

[44] M. Hemmer, A. Vaupel, and M. Richardson, "Current status of the HERACLES, a millijoule level, multi kHz, few-cycle, and CEP stabilized OPCPA system," in *Lasers and Electro-Optics (CLEO) and Quantum Electronics and Laser Science Conference (QELS), 2010 Conference on*, 2010), 1-2.

[45] M. Hemmer, A. Vaupel, B. Webb, and M. Richardson, "Multi-kHz, multi-mJ, phase stabilized, OPCPA amplifier system," in *SPIE Solid State Lasers XIX: Technology and Devices*, 2010), 757818-757818.

[46] M. Hemmer, A. Vaupel, M. Wohlmuth, and M. Richardson, "OPCPA pump laser based on a regenerative amplifier with volume Bragg grating spectral filtering," Applied Physics B **106**, 599-603 (2012).

[47] D. S. Sumida and T. Y. Fan, "Effect of radiation trapping on fluorescence lifetime and emission cross section measurements in solid-state laser media," Optics Letters **19**, 1343-1345 (1994).